NASA TN D-154

TECHNICAL NOTE

D-154

BRAKING AND LANDING TESTS ON SOME NEW TYPES OF AIRPLANE LANDING MATS AND MEMBRANES

By Sidney A. Batterson

Langley Research Center
Langley Field, Va.

NATIONAL AERONAUTICS AND SPACE ADMINISTRATION

WASHINGTON October 1959

NATIONAL AERONAUTICS AND SPACE ADMINISTRATION

TECHNICAL NOTE D-154

BRAKING AND LANDING TESTS ON SOME NEW TYPES OF AIRPLANE LANDING MATS AND MEMBRANES

By Sidney A. Batterson

SUMMARY

An experimental investigation was made at the Langley landing-loads track to obtain friction coefficients developed during braking and landing on various types of metal landing mats and prefabricated membranes. The tests were made at forward speeds of about 85 knots with static vertical loads of 20,405 and 13,020 pounds. The results indicated the effect of each type of mat and membrane on the variation of the coefficient of friction. Braking tests were made for both dry and wet surface conditions.

INTRODUCTION

The armed services are currently engaged in a program directed toward improving the pierced-steel landing mats now in use for converting unprepared areas into landing strips for aircraft. During the take-off of jet airplanes, the holes in these mats (see fig. 1) are the source of large amounts of dust and foreign particles which are ingested into the jet engines. The dust is also a visual handicap and sometimes causes serious delays in subsequent airplane take-offs.

Several methods for solving this problem are being investigated. One method is to eliminate the holes by using unpierced mats; another method is to place a waterproof prefabricated membrane between a pierced type of metal mat and the ground. Since the membranes are considerably lighter and more flexible than the metal landing mats, it would be desirable to operate off the membranes alone in areas where the ground has sufficient bearing strength. In order to determine the effect of the various types of metal landing mats and membranes on the landing and taxiing operations of aircraft, simulated landing and braking tests were made at the Langley landing-loads track. The purpose of this investigation is to show the effect of the various types of landing mats and membranes on the braking and spin-up drag coefficients of friction. These tests were made with a jet-airplane landing gear having

a static-load rating of 20,000 pounds. The tests were made at forward speeds of around 85 knots under both wet and dry conditions.

DESCRIPTION OF METAL LANDING MATS AND MEMBRANES USED FOR TESTS

This investigation was carried out with five types of metal landing mats (figs. 1 to 5) and four types of prefabricated membranes (figs. 6 to 9). Figures 1 to 3 show the pierced type of landing mats with their approximate dimensions. Mat M9 is fabricated of aluminum and mats M8 and M6 are made of steel. The unpierced metal landing mats are shown in figures 4 and 5; mat T8 is fabricated of magnesium and mat T10 of steel. The T14 membrane (fig. 6) is made of nylon coated with neoprene and has an embossed surface finish. Membrane T13 (fig. 7) is made of nylon and is coated with vinyl and has a smooth finish. Membrane T12 (fig. 8) is made of nylon coated with neoprene and has a smooth surface finish. Membrane T1 (fig. 9) is made of cotton duck coated with a smooth vinyl finish.

APPARATUS AND TEST PROCEDURE

The tests were made by simulating actual landings and braked taxiing runs on the metal landing mats and prefabricated membranes at the Langley landing-loads track. The basic elements of this facility are shown schematically in figure 10. Included is a large main carriage (fig. 11) weighing approximately 100,000 pounds traveling on steel rails which are located on each side of a 2,200-foot-long concrete runway. The tests were made on 50-foot lengths of the mats and membranes which were clamped onto the runway surface. Figure 12 shows a typical mat installation and figure 13 shows a typical membrane installation.

The landing gear used for these tests was the main gear of a jet airplane. It was equipped with a ribbed tread 44 × 13, type VII, 26-ply-rating tire (fig. 14). The tire inflation pressure was 200 pounds per square inch for all tests. The wheel was equipped with a hydraulic disk-type brake having a maximum specified operating pressure of 1,050 pounds per square inch. During these tests it was necessary to exceed this pressure by about 10 percent in order to develop the maximum coefficients of friction. The tests were made with the landing-gear strut inclined at an angle of 15° (nose up) to the vertical. The yaw and roll angles were 0° throughout the entire investigation.

The landing gear was attached to the drop carriage located within the main carriage (fig. 14). Motion of the drop carriage with respect to the main carriage is restrained so that it travels only in the vertical direction. Landing impacts were made by accelerating the main carriage to the desired forward speed of about 85 knots by means of the hydraulic jet catapult (ref. 1) and then releasing the drop carriage which was initially set at the height necessary to develop a vertical velocity of approximately 9 feet per second at impact. Just prior to the instant of touchdown, a hydraulic engine applied a lift force equal to the dropping weight to simulate a wing lift force of 1 g throughout the landing impact.

The braked taxiing tests were made by accelerating the carriage to the desired forward speed and then placing the landing gear on the runway well ahead of the mat or membrane specimen being tested. For the braking tests no wing lift was applied and the wheel was allowed to roll freely under the static vertical load. As the wheel rolled onto the mat the brakes were applied.

Braked taxiing tests and landing-impact tests were made on each of the mats and the membranes. One group of braked taxiing tests was made with the mat and membrane surfaces dry. Another group of tests was made immediately after water had been splashed on the mats and membranes to simulate the surface conditions existing during rainy weather. All landing-impact tests were made on dry surfaces. The metal landing mats were installed with the male portion of the locking devices pointed toward the approaching landing gear. (See figs. 1 to 5.) During the braking tests, with a static vertical load of 20,405 pounds, sufficient brake torque was available to achieve a locked-wheel skid before the end of mat or membrane was reached during all tests except for the dry-surface tests of the metal landing mats and the T14 membrane. For the dry-surface braking tests of these specimens, weight was removed from the drop carriage and tests were made with a static vertical load of 13,020 pounds. With this loading condition, sufficient brake torque was available either to lock the wheel or to reach a slip ratio well beyond that at which the maximum coefficient of friction was developed, before the end of the mat or membrane was reached. Although operating at a reduced weight caused a reduction in the tire-footprint area, this reduction was not believed to affect significantly the magnitude or variation of the coefficient of friction.

INSTRUMENTATION

Instrumentation was provided to obtain the vertical and drag force developed between the tire and runway, the landing-gear wheel velocity, and the brake pressure. Figure 15 is a schematic drawing of the test apparatus and shows the locations of most of the instruments.

The methods used for measuring the vertical and spin-up drag loads developed during the landing impact are the same as those described in reference 2. The vertical load was obtained from the dynamometer (fig. 15) with corrections applied for the inertia forces introduced by the masses below the dynamometer. During the landing tests the spin-up drag load was derived from the wheel angular acceleration and tire-deflection measurements. During the braking tests, the angular accelerometer method could not be used to obtain drag loads because of the presence of the unknown applied brake torque; therefore, braked ground drag loads were obtained from the drag component of the dynamometer with corrections applied for the inertia forces developed in the drag direction. The drag component of the dynamometer and the horizontal accelerometers used for finding the magnitude of the inertia forces between the runway surface and the dynamometer are indicated in figure 15. A typical time-history plot of the drag component of the dynamometer as well as the ground drag load obtained by applying corrections for the inertia forces developed by the masses below the dynamometer is shown in figure 16. Since some oscillations remained in the latter curve, it appeared that the corrections did not completely account for the inertia effects of the masses below the dynamometer. Therefore, the data used for this investigation were obtained from a curve faired through the ground drag plot as shown in figure 16. The wheel angular velocity was obtained from the same voltage generator used for the tests described in reference 2. The horizontal velocity of the main carriage was obtained by noting the time required to travel a given distance (ref. 2). The pressure in the wheel-brake hydraulic system was measured with a strain-gage-type pressure gage.

RESULTS AND DISCUSSION

Braked Taxiing Tests

The conditions for each of the braked taxiing tests are listed in table I. Figure 17 shows time histories of the applied wheel brake pressure, wheel angular velocity, and ground drag load obtained during a typical braking test. The brake pressure and angular velocity are direct plots of the outputs of the pressure gage and velocity generator. The drag curve, however, is the faired value obtained after correcting the dynamometer drag load for the upper and lower mass inertia reactions. (See fig. 16.)

Figure 18 shows the results of the dry-surface braking tests made on all five of the metal landing mats. The coefficient of friction obtained during each test is plotted against the slip ratio. Slip

ratio is defined as $\frac{\omega - \omega_b}{\omega}$ where

ω angular velocity of wheel if rolling free

ω_b angular velocity of wheel during braking

It is apparent from this definition that a slip ratio of 0 indicates a freely rolling wheel and a slip ratio of 1.0 indicates that the wheel is locked. It can be seen in figure 18 that, as the brakes are applied, the coefficient of friction increases rapidly with slip ratio and reaches a peak in the range of slip ratios lying between 0.1 and 0.2. This is the practical range of the curves, since if effective and stable braking is to be obtained, the wheel must operate at slip ratios associated with this rising slope. If the brake torque applied is sufficient to cause the wheel to operate at slip ratios larger than those for the peak coefficient of friction, the operation becomes unstable and the wheel locks quickly, and results in a large decrease in the coefficient of friction. During these tests the time between the peak and the locking of the wheel was less than 0.1 second. (See, for example, fig. 17.) For the runs in figure 18 it can be seen that the highest coefficient of friction was slightly greater than 0.7 and was obtained on the unpierced T8 mat. This peak value is almost as large as that indicated by some unpublished data obtained during braking tests made on concrete for similar speeds and tire pressures. It should be pointed out that the forward speed recorded for the braked test on the T8 mat was somewhat lower than that for the other braked runs. (See table I.) Although a decrease in forward speed causes an increase in friction coefficient (see, for example, refs. 2 and 3), this difference should not be enough to change materially the relationship of the curves in figure 18. The lowest peak coefficient of friction, which was slightly greater than 0.5, was obtained on the unpierced T10 mat. The T8 and the T10 mats, in addition to having different cross-sectional shapes (compare fig. 4 with fig. 5), also had different surface finishes. Mat T8 had a dull finish and mat T10 had a smooth glossy finish. It is not known how much each of these differences in the mats contributed to the significantly lower coefficient on the T10 mat. The results of the tests made on the pierced mats (figs. 1 to 3), which had similar surface finishes, showed only small differences in the friction values. This result indicates that the differences in cross section (primarily the hole size and mat thickness) had very little effect on the friction properties of the pierced mats. Figure 18 also indicates that the locked-wheel sliding coefficient of friction for all of the dry-surface metal landing mats is in the neighborhood of 0.2 to 0.3.

Figure 19 shows the results which were obtained when water was splashed on the metal landing mats just before the test in order to simulate operations during rainy weather. It is apparent that wetting

the mats caused a very large decrease in the coefficient of friction. On the average, the maximum coefficients obtained for the wet mats were about one-third of the values obtained on the dry mats. It can be seen in figure 19 that, with the exception of the T8 mat, all mats gave stable coefficient-of-friction variations; that is, friction coefficient increased in value with slip ratio. The reason for this difference in the results obtained with the T8 mat is not known. However, in addition to its difference in shape and surface finish, which was indicated earlier, it should be pointed out that the water on its surface collected to a depth level with the small ridges (fig. 4) whereas on the other mats the bulk of the water drained off the surface and what remained either collected in large globules or just wetted the surface.

In an effort to find some method for increasing the coefficient of friction obtained on the wet surfaces, a nonskid compound consisting of a gritty substance suspended in a binder capable of adhering to the mat surface was painted onto the T10 mat. The results of braking tests made on this surface are shown in figure 20. These results indicate that coating the mats with a gritty, nonskid compound causes large increases in the coefficient of friction for both wet and dry conditions on this landing mat. The coated mat, when wet, develops slightly higher coefficients of friction than the dry, uncoated mat, and the coated mat, when dry, develops friction coefficients almost as high as expected on dry concrete.

Figure 21 shows the results of the braking tests made on the dry membranes. It can be seen that the T14 membrane exhibited by far the highest coefficient of friction. This membrane had an embossed surface as contrasted with the smooth surfaces of the other membranes. These data indicate that, for dry braking, a roughened membrane surface tends to increase the coefficient of friction. Figure 21 also shows that the vinyl covered T1 and T13 membranes developed approximately the same coefficients whereas the neoprene covered T12 membrane developed substantially smaller coefficients. This indicates that a smooth finish vinyl coating is capable of developing higher braking coefficients than a smooth neoprene finish.

Figure 22 shows that wetting down the membranes causes very large reductions in the braking coefficients of friction. The maximum coefficients obtained were in the neighborhood of 0.1 or less. These coefficients are so low that the differences in surface material and surface finish are of no practical importance when the membranes are wet.

Landing-Impact Tests

The conditions for the landing-impact tests made on each of the metal landing mats and membranes are given in table II. The results

obtained from these tests are shown in figures 23 to 31. For the metal landing mats, the coefficients of friction and resulting drag forces were high enough to allow the wheel to achieve full rolling velocity before reaching the end of the mat. For all membranes except the T14 membrane, the wheel rolled off the end of the mat before reaching full rolling velocity. This result is in agreement with results obtained in the braking tests, which showed that the highest coefficients of friction were developed on the metal landing mats and the T14 membrane. A comparison of the spin-up drag coefficients of friction obtained during these tests made on the landing mats and membranes with those obtained during the landing-impact tests made on concrete and reported in reference 2 shows that the coefficients developed on the metal landing mats and membranes were significantly smaller. Furthermore, the spin-up drag coefficients obtained during these tests on the mats and membranes are much less than the maximum coefficients developed during the braking tests. This result would suggest conditions similar to those found in reference 2 wherein molten rubber in the tire-footprint area at the time of wheel spin-up caused reductions in the maximum coefficients of friction. This would further indicate that the coefficient of friction that can be developed during the period in which the tire footprint contains molten rubber is much less for landings on the metal landing mats and membranes than for landings on concrete.

SUMMARY OF RESULTS

A series of braked taxiing and landing-impact tests made over five types of metal landing mats and four types of prefabricated membranes gave the following results:

1. For the dry-surface braking tests of the metal landing mats, mat T8 developed the highest coefficient of friction (about 0.7) and mat T10 the lowest (about 0.5). The values of the coefficients developed by the other three metal mats showed only small differences.

2. The locked-wheel sliding coefficient of friction for all the dry-surface metal landing mats was in the neighborhood of 0.2 to 0.3.

3. The maximum coefficients of friction developed during braked taxiing runs over the wet metal landing mats were, on the average, about one-third as large as those obtained on the dry mats.

4. A coating of a nonskid compound painted on the T10 mat resulted in large increases in the braking coefficient of friction for both wet and dry surface conditions.

5. For the dry-surface braking tests of the membranes, the smooth finish vinyl coated membranes developed higher coefficients of friction than the smooth finish neoprene; however, the highest coefficient was developed on the embossed neoprene-coated membrane.

6. The presence of water on the membrane surface caused very large reductions in the braking coefficients of friction.

7. The spin-up drag coefficients of friction obtained during the landings made on the metal landing mats and the prefabricated membranes were significantly smaller than those obtained during landings made on concrete.

Langley Research Center,
National Aeronautics and Space Administration,
Langley Field, Va., August 6, 1959.

REFERENCES

1. Joyner, Upshur T., and Horne, Walter B.: Considerations on a Large Hydraulic Jet Catapult. NACA TN 3203, 1954. (Supersedes NACA RM L51B27.)

2. Batterson, Sidney A.: Investigation of the Maximum Spin-up Coefficients of Friction Obtained During Tests of a Landing Gear Having a Static-Load Rating of 20,000 Pounds. NASA MEMO 12-20-58L, 1959.

3. Westfall, John R., Milwitzky, Benjamin, Silsby, Norman S., and Dreher, Robert C.: A Summary of Ground-Loads Statistics. NACA TN 4008, 1957.

TABLE I

CONDITIONS FOR BRAKED TAXIING TESTS

Test	Test specimen	Horizontal velocity, ft/sec	Static vertical load, lb	Surface condition
1	T10 mat	143	13,020	Dry
2	T10 mat	133	20,405	Wet
3	T10 mat	145	13,020	Wet
4	T8 mat	120	13,020	Dry
5	T8 mat	144	20,405	Wet
6	M9 mat	146	13,020	Dry
7	M9 mat	146	20,405	Wet
8	M8 mat	138	13,020	Dry
9	M8 mat	148	20,405	Wet
10	M6 mat	138	13,020	Dry
11	M6 mat	138	20,405	Wet
12	T10 mat[a]	138	13,020	Dry
13	T10 mat[a]	144	13,020	Wet
14	T14 membrane	144	13,020	Dry
15	T14 membrane	138	20,405	Wet
16	T13 membrane	134	20,405	Dry
17	T13 membrane	138	20,405	Wet
18	T12 membrane	144	20,405	Dry
19	T12 membrane	145	20,405	Wet
20	T1 membrane	138	20,405	Dry
21	T1 membrane	142	20,405	Wet

[a]Mat surface coated with nonskid compound.

TABLE II

CONDITIONS FOR LANDING-IMPACT TESTS

Test	Test specimen	Horizontal velocity, ft/sec	Vertical velocity, ft/sec
22	T10 mat	139	9.0
23	T8 mat	140	9.5
24	M9 mat	130	9.2
25	M8 mat	129	9.1
26	M6 mat	130	9.2
27	T14 membrane	128	9.4
28	T13 membrane	125	9.1
29	T12 membrane	134	8.7
30	T1 membrane	137	9.4

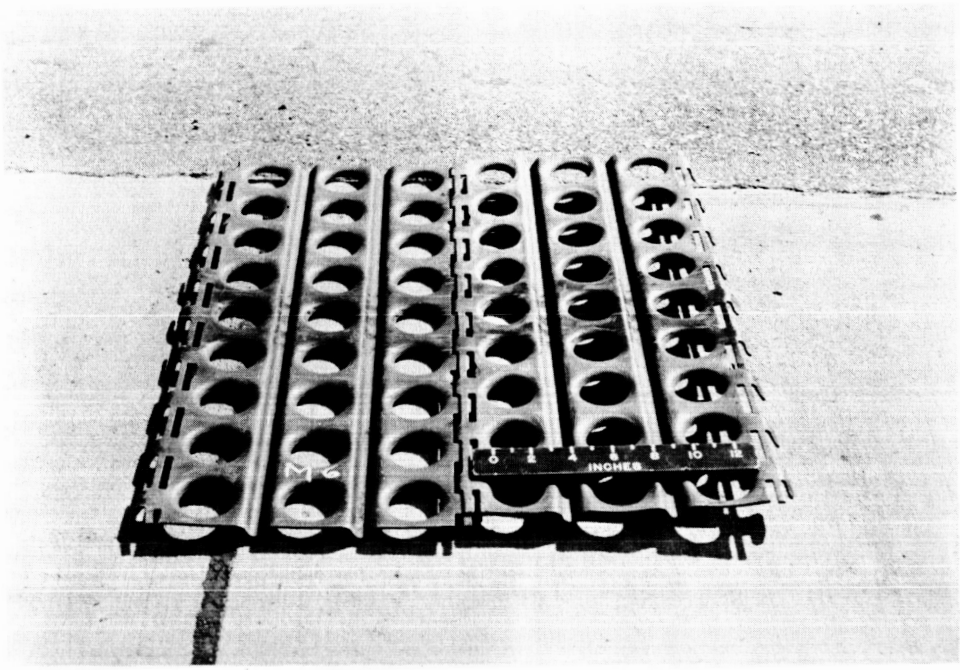

L-59-2084

(a) Photograph of joined mat sections; landing-gear travel was from left to right during tests.

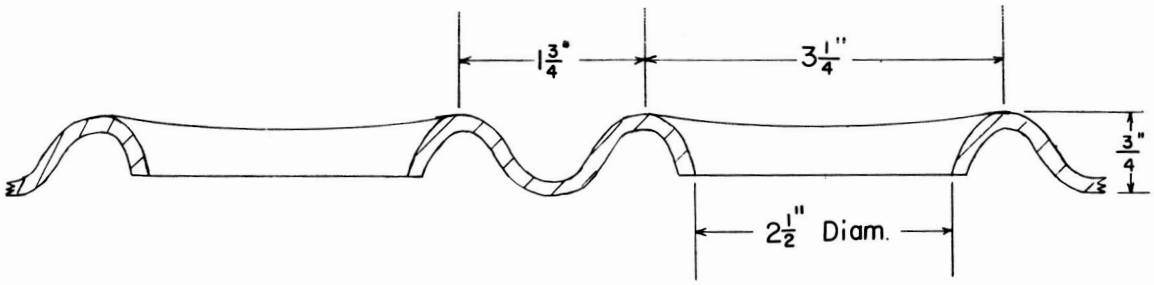

(b) Cross-sectional view of landing mat.

Figure 1.- Photograph and approximate dimensions of M6 steel landing mat.

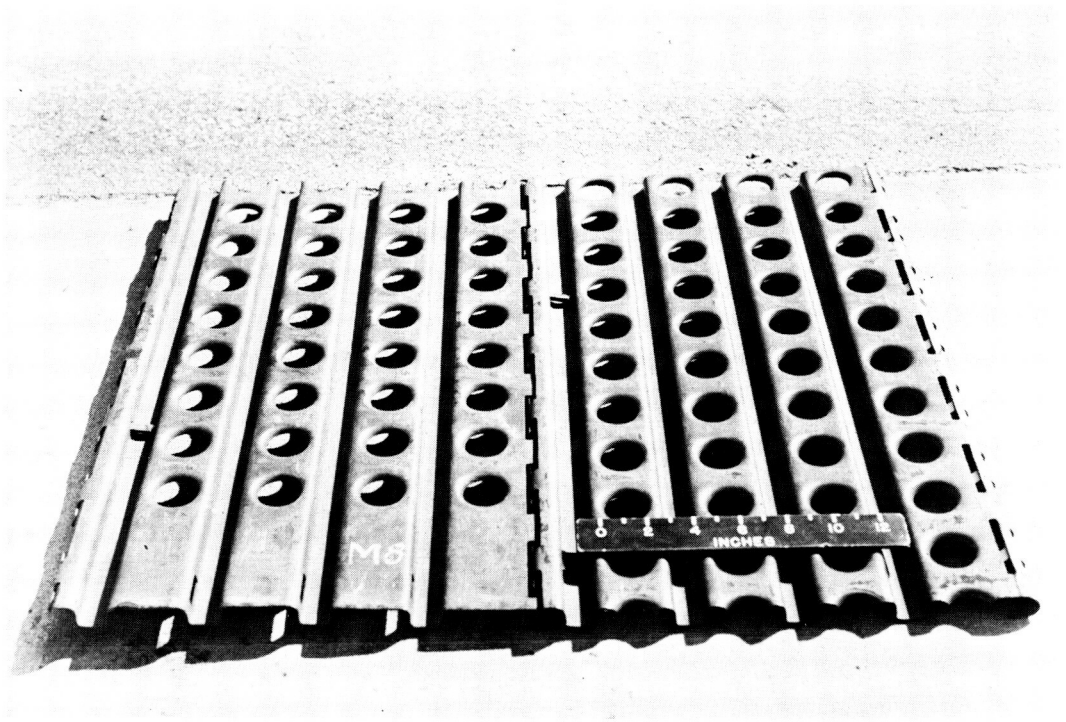

L-59-2088

(a) Photograph of joined mat sections; landing-gear travel was from left to right during tests.

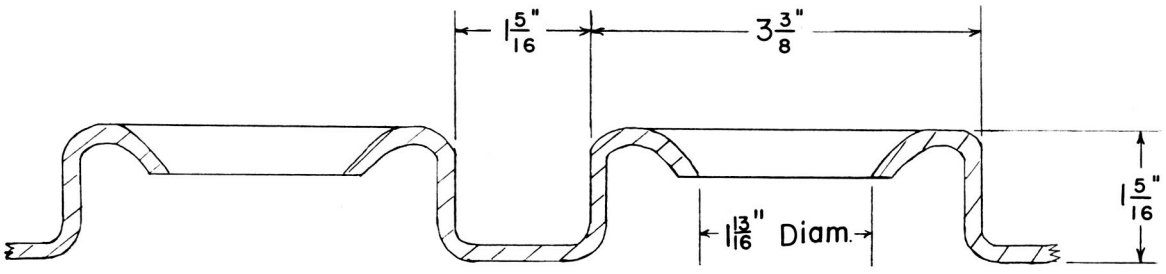

(b) Cross-sectional view of landing mat.

Figure 2.- Photograph and approximate dimensions of M8 steel landing mat.

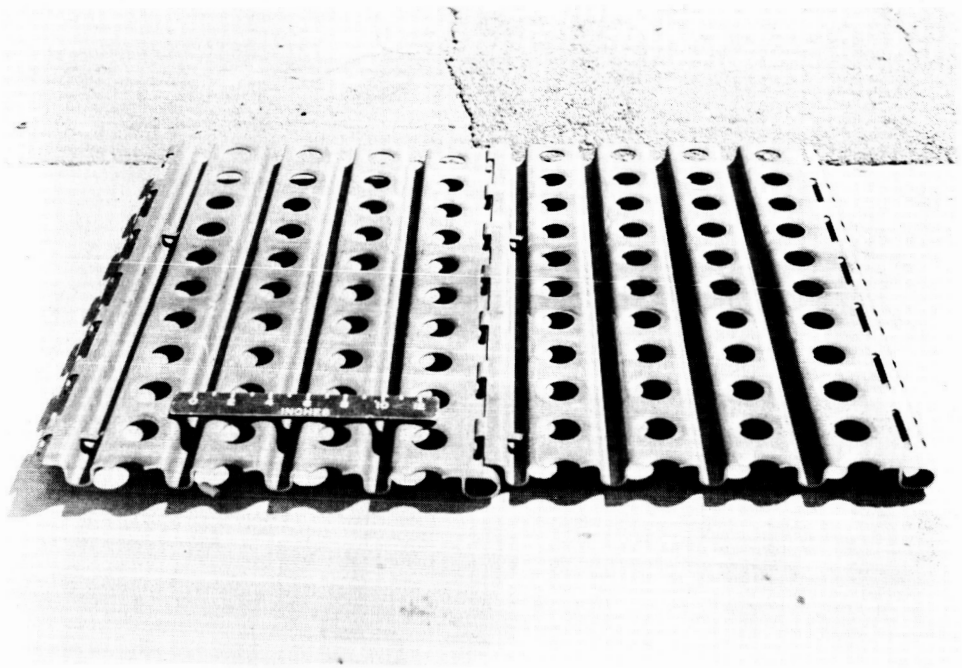

L-59-2083

(a) Photograph of joined mat sections; landing-gear travel was from left to right during tests.

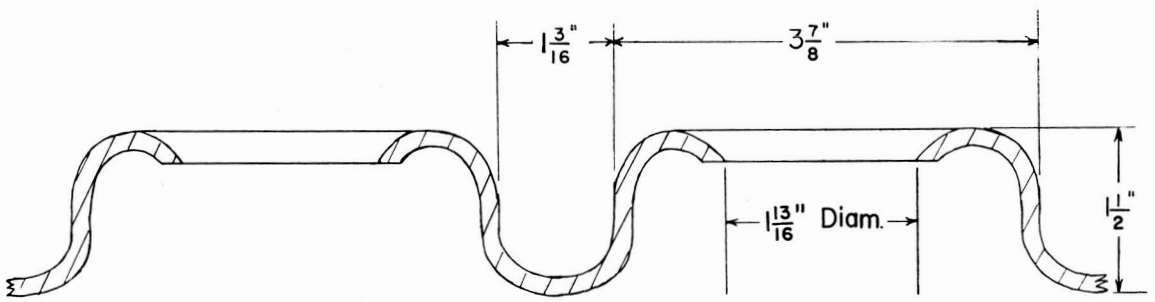

(b) Cross-sectional view of landing mat.

Figure 3.- Photograph and approximate dimensions of M9 aluminum landing mat.

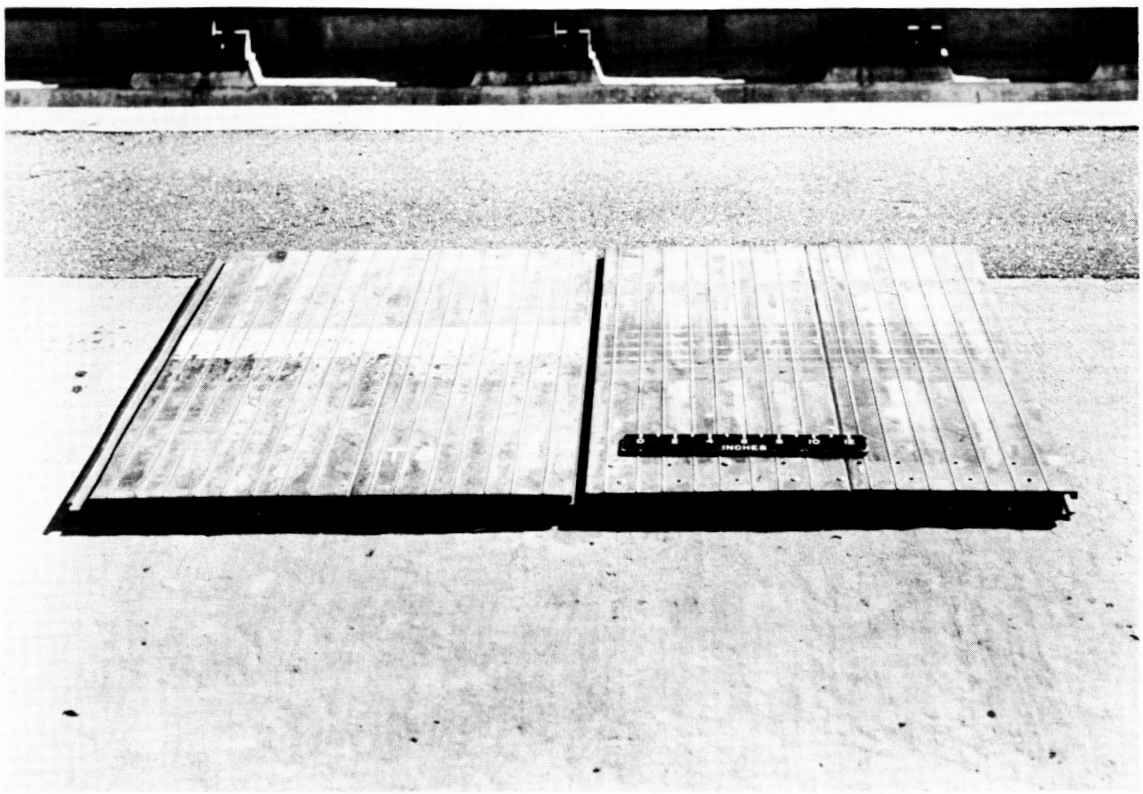

L-59-2085

(a) Photograph of joined mat sections; landing-gear travel was from left to right during tests.

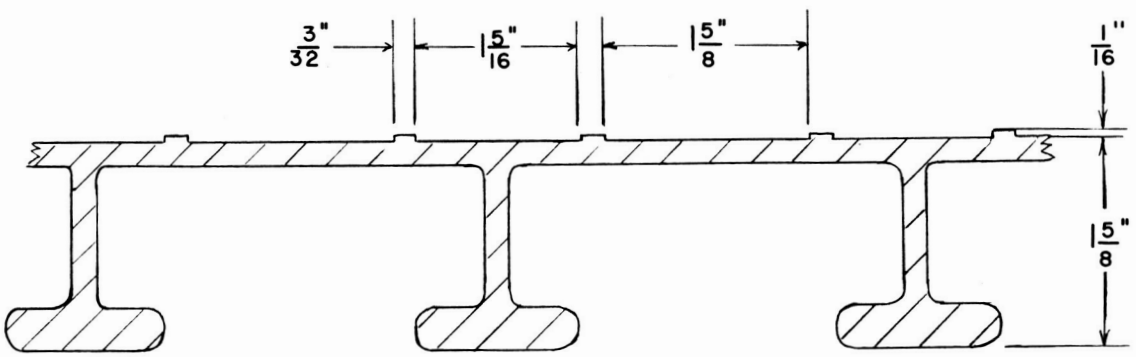

(b) Cross-sectional view of landing mat.

Figure 4.- Photograph and approximate dimensions of T8 magnesium landing mat.

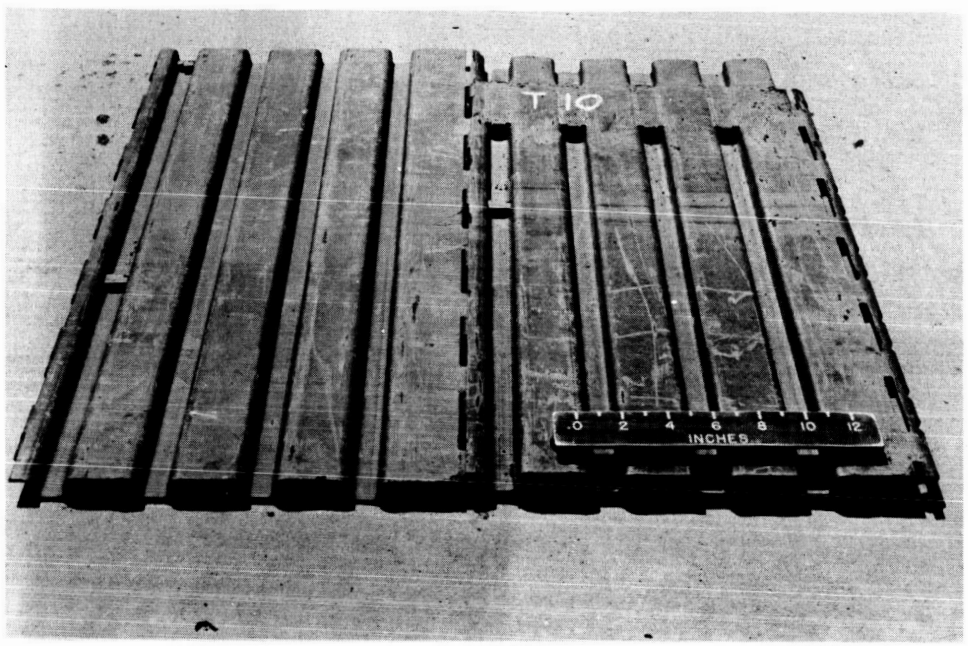

L-59-3137

(a) Photograph of joined mat sections; landing-gear travel was from left to right during tests.

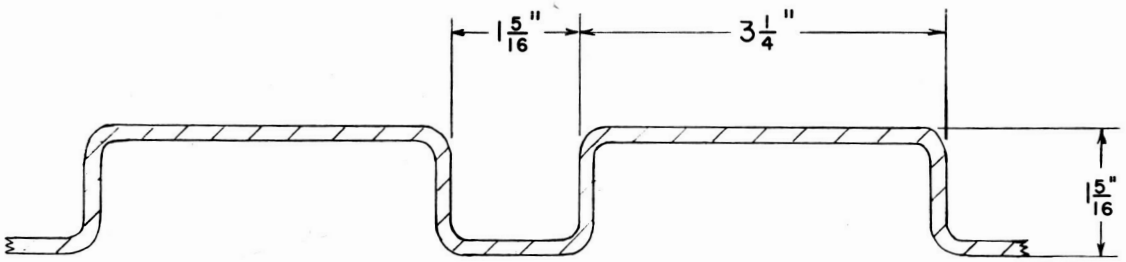

(b) Cross-sectional view of landing mat.

Figure 5.- Photograph and approximate dimensions of T10 steel landing mat.

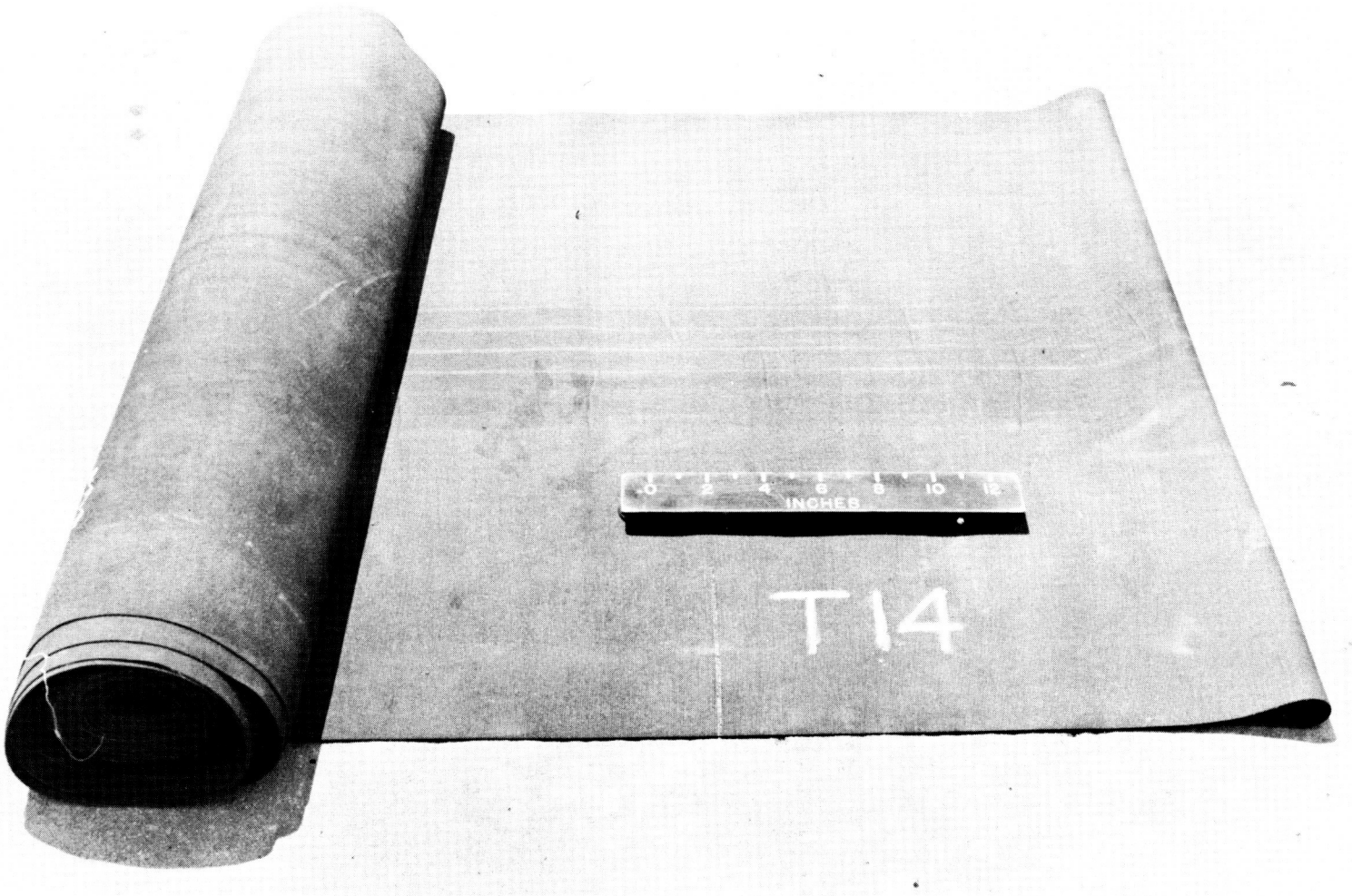

Figure 6.- Photograph of prefabricated membrane T14. L-59-3139

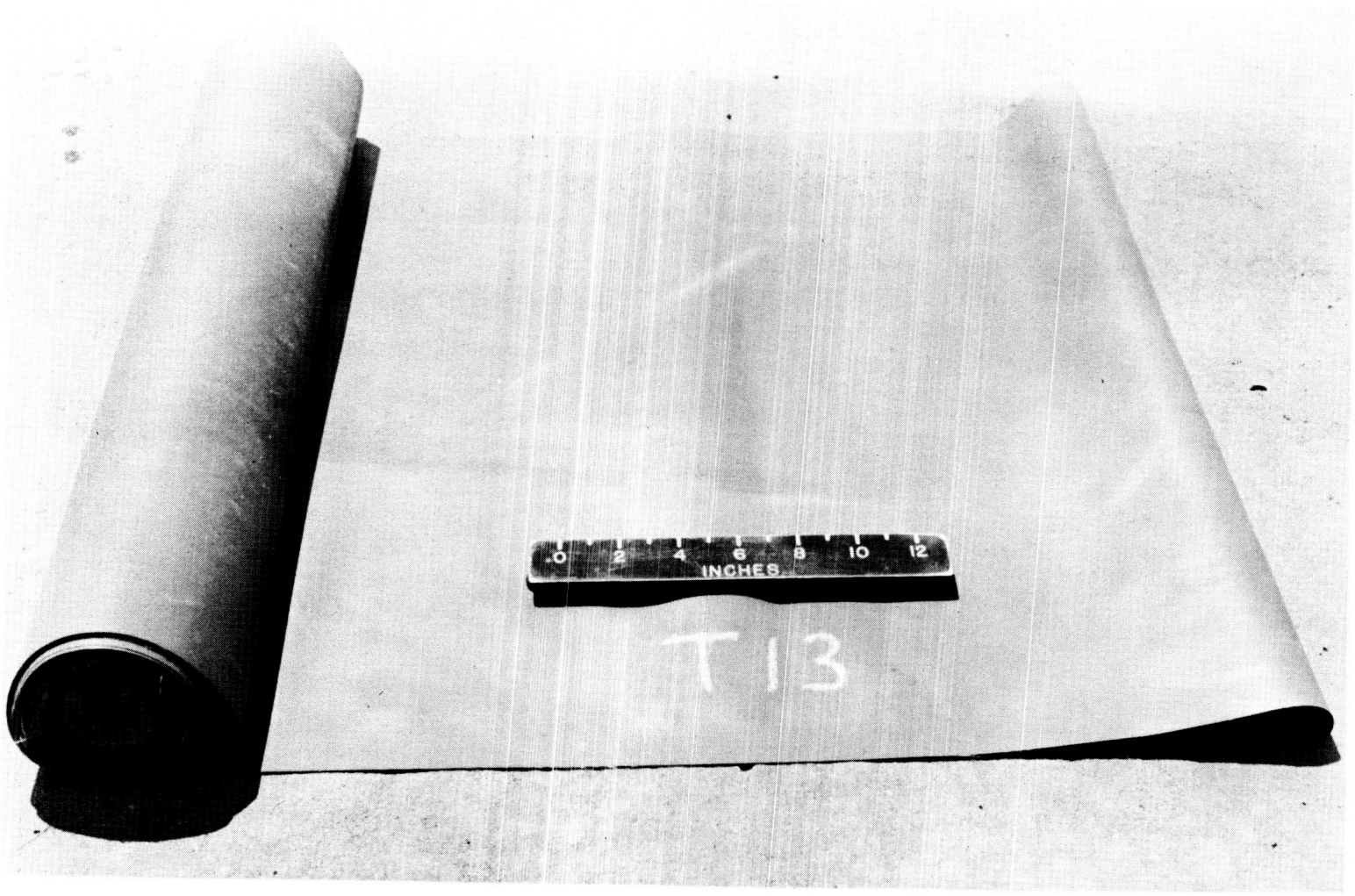

Figure 7.- Photograph of prefabricated membrane T13. L-59-3138

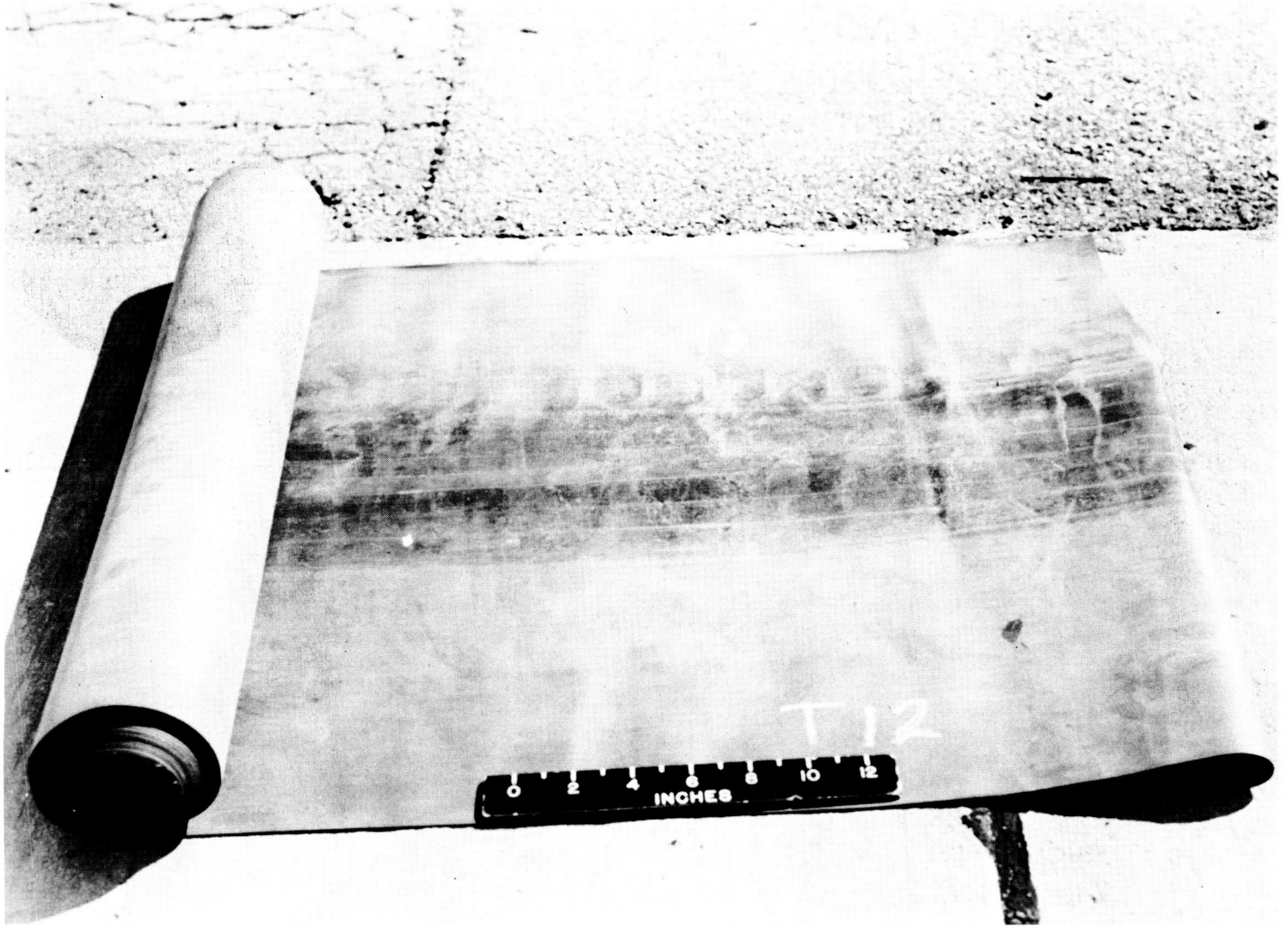

Figure 8.- Photograph of prefabricated membrane T12. L-59-2090

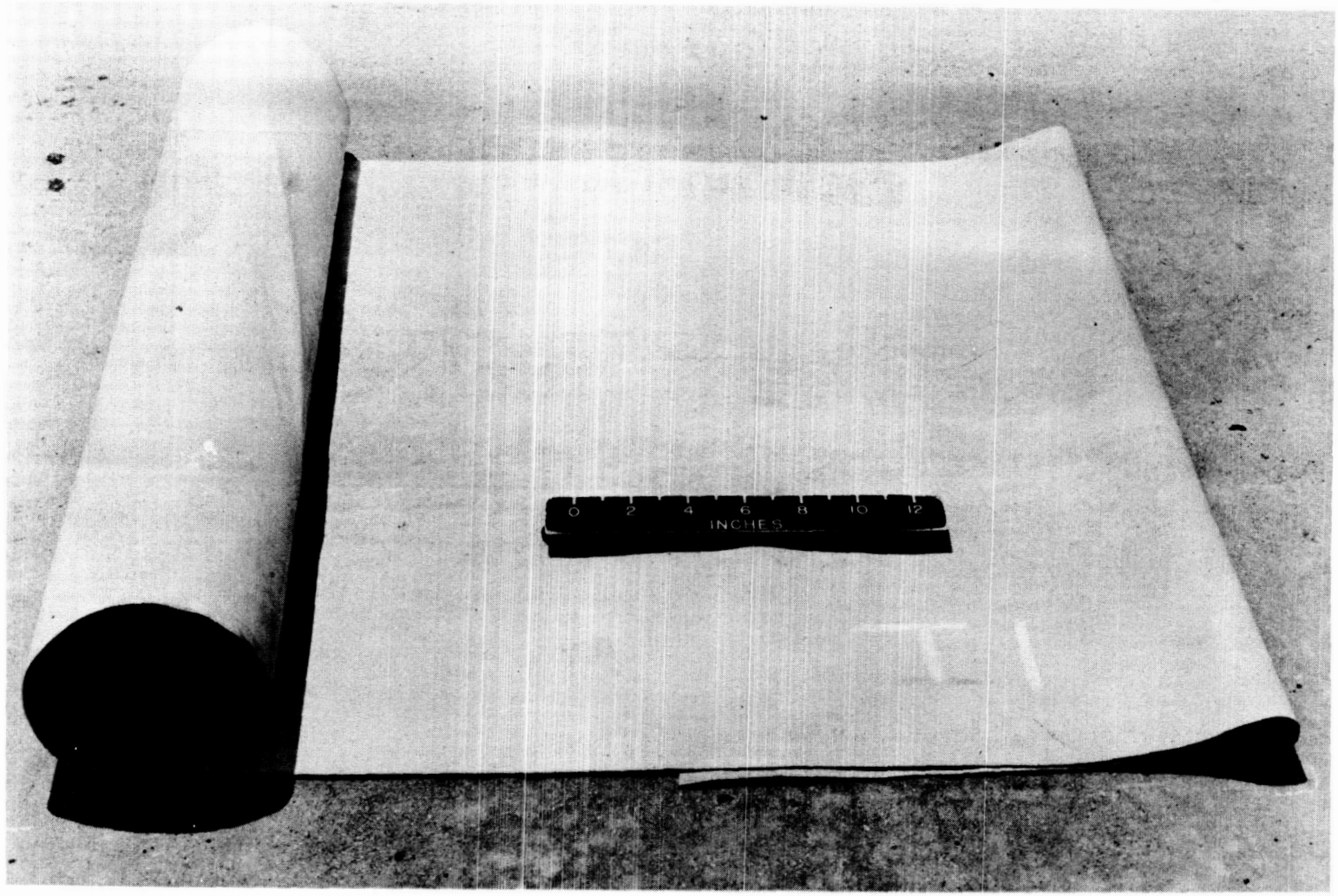

Figure 9.- Photograph of prefabricated membrane T1. L-59-3136

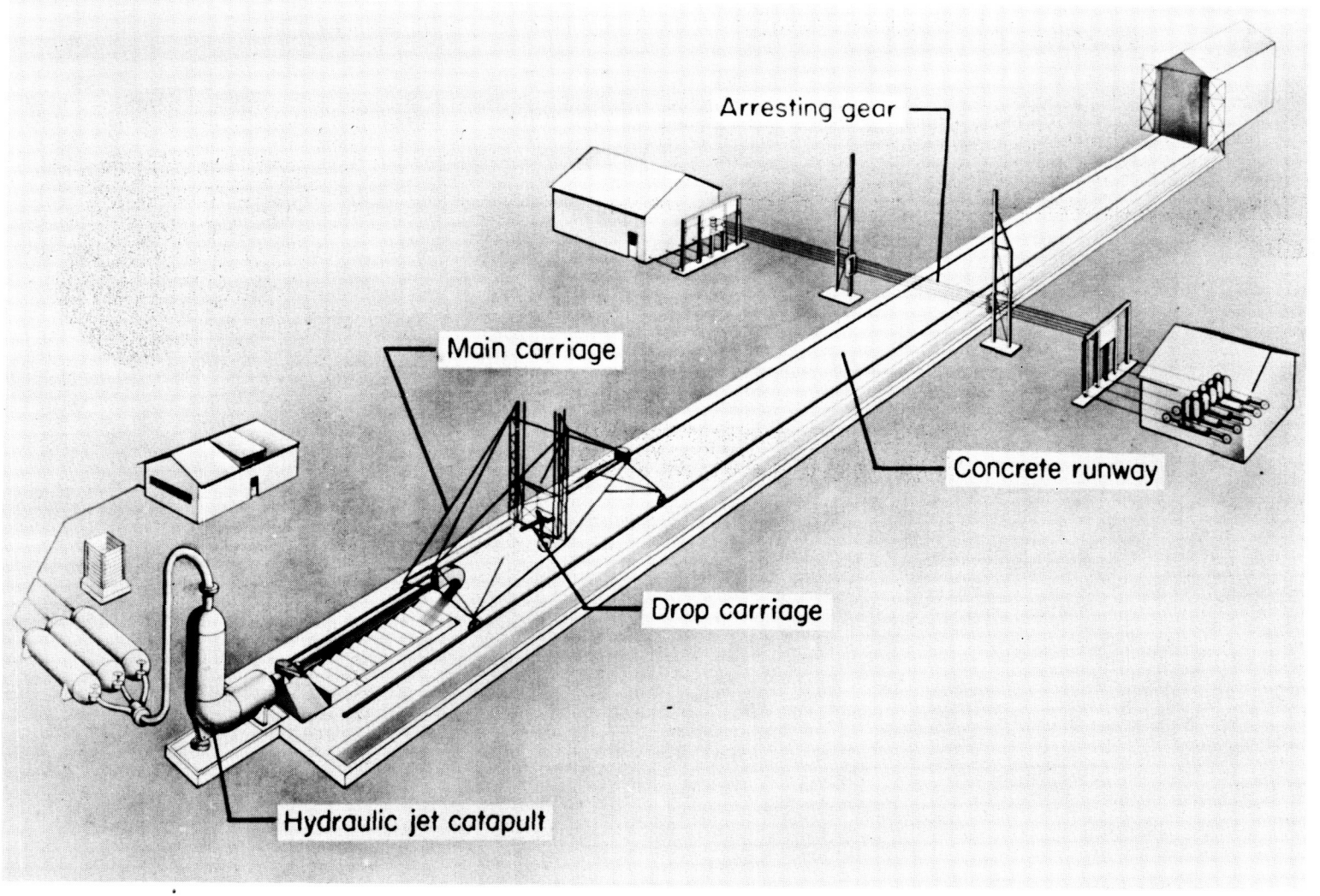

L-58-1693

Figure 10.- Schematic drawing of Langley landing-loads track.

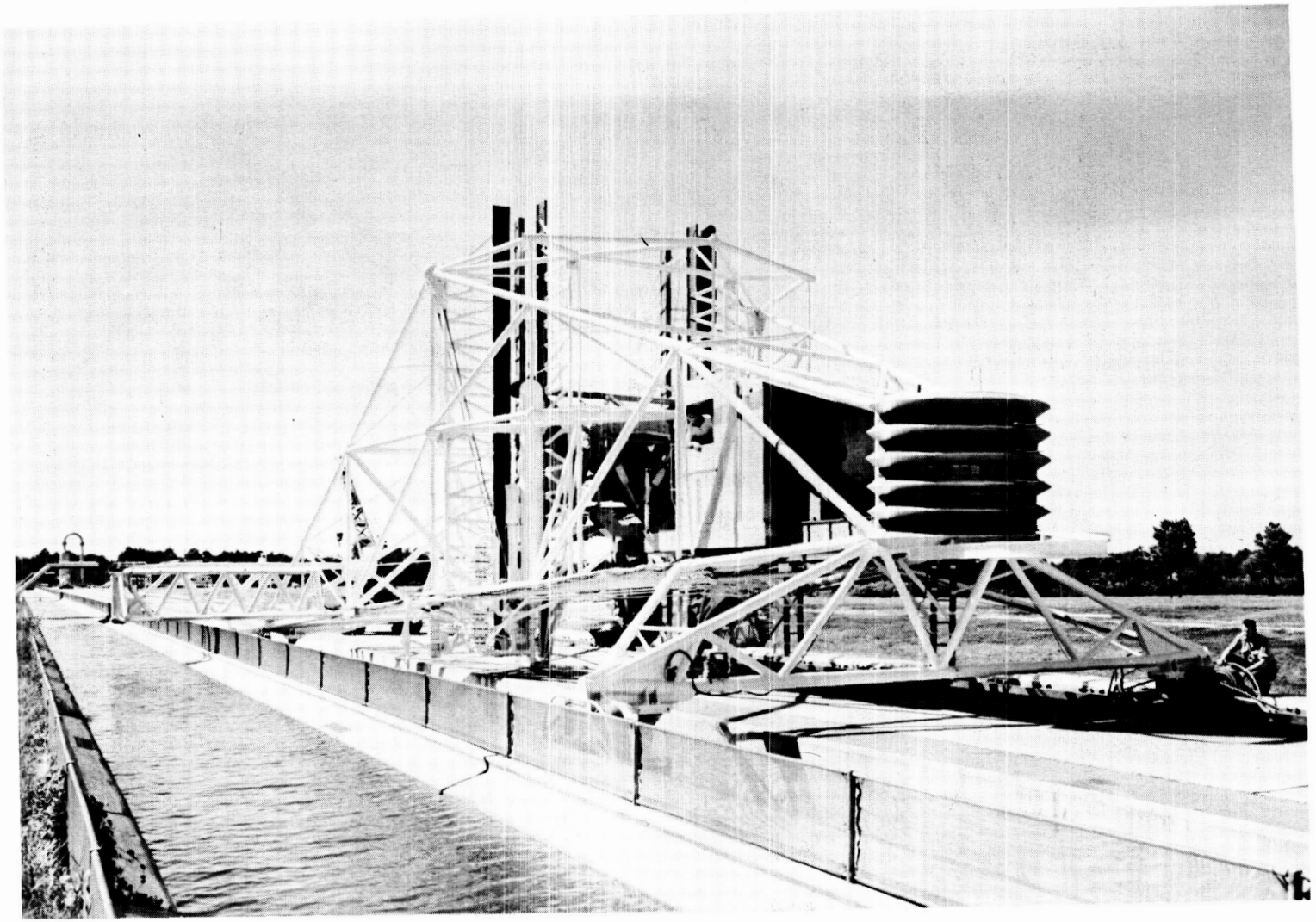

Figure 11.- Langley landing-loads track carriage. L-95476

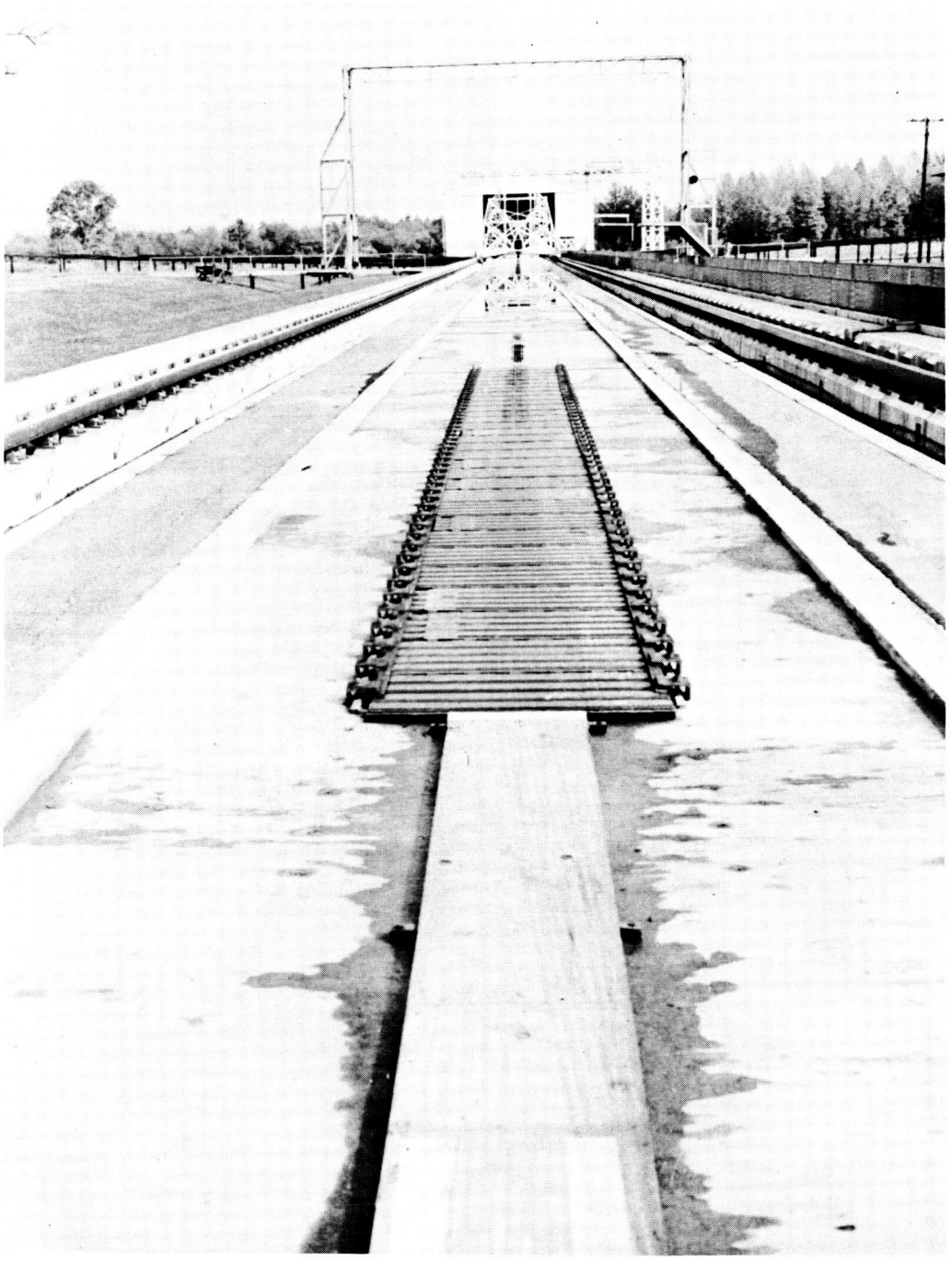

L-58-737a

Figure 12.- Installation of T10 landing mat at Langley landing-loads track.

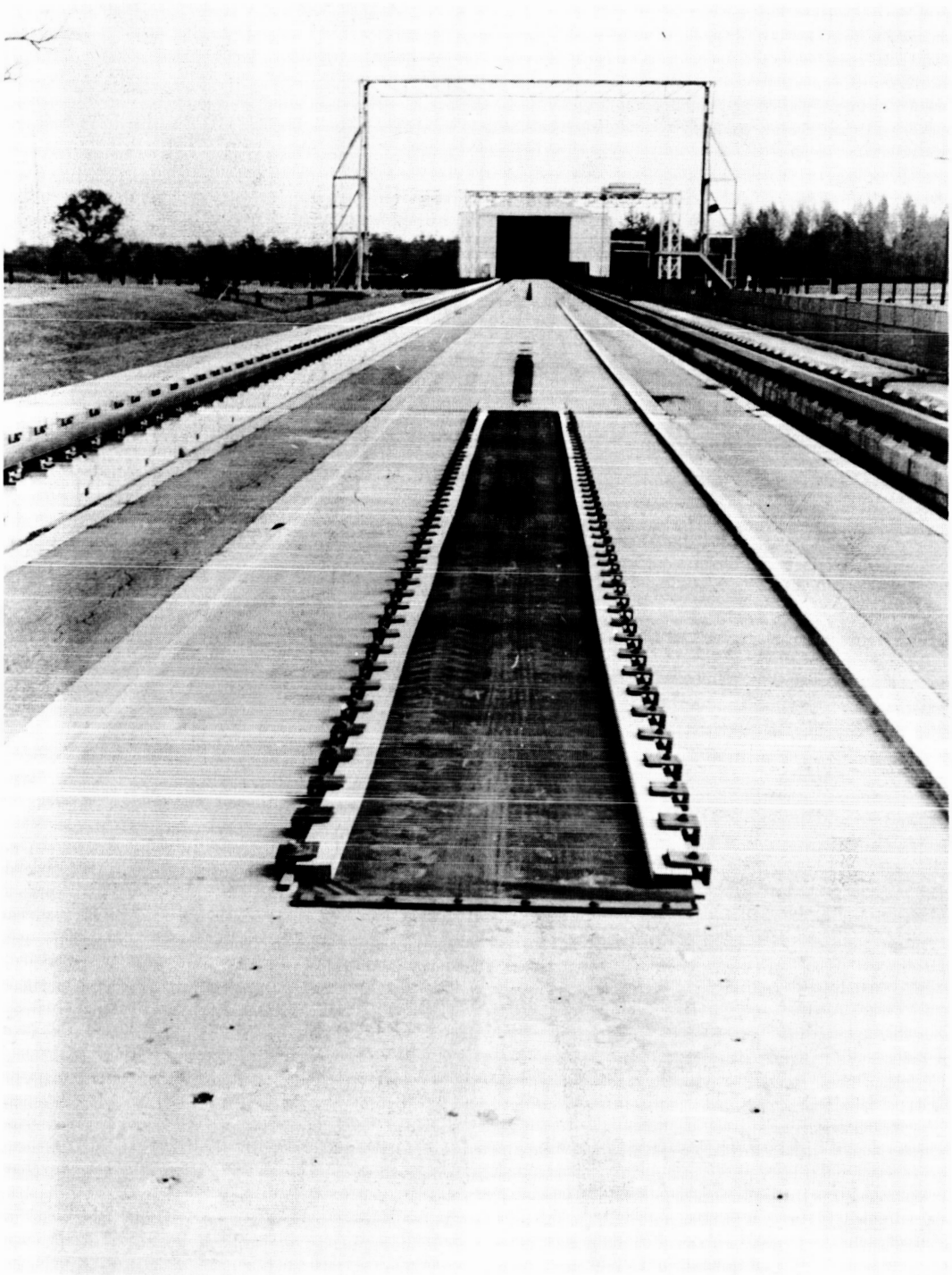

L-58-664a

Figure 13.- Installation of T14 membrane at Langley landing-loads track.

Figure 14.- Landing gear mounted for testing. L-57-1338

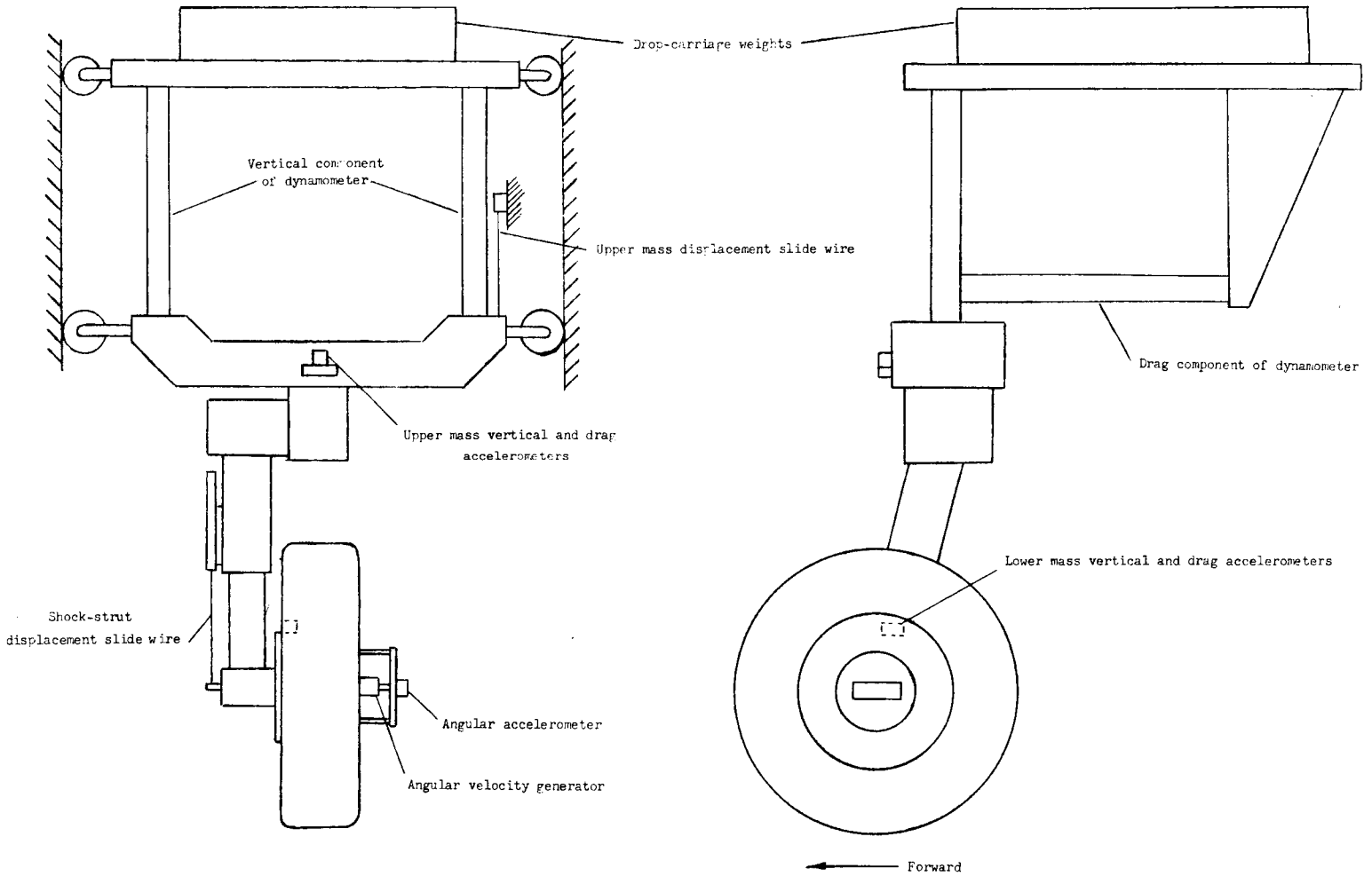

Figure 15.- Schematic view of landing gear and instrumentation.

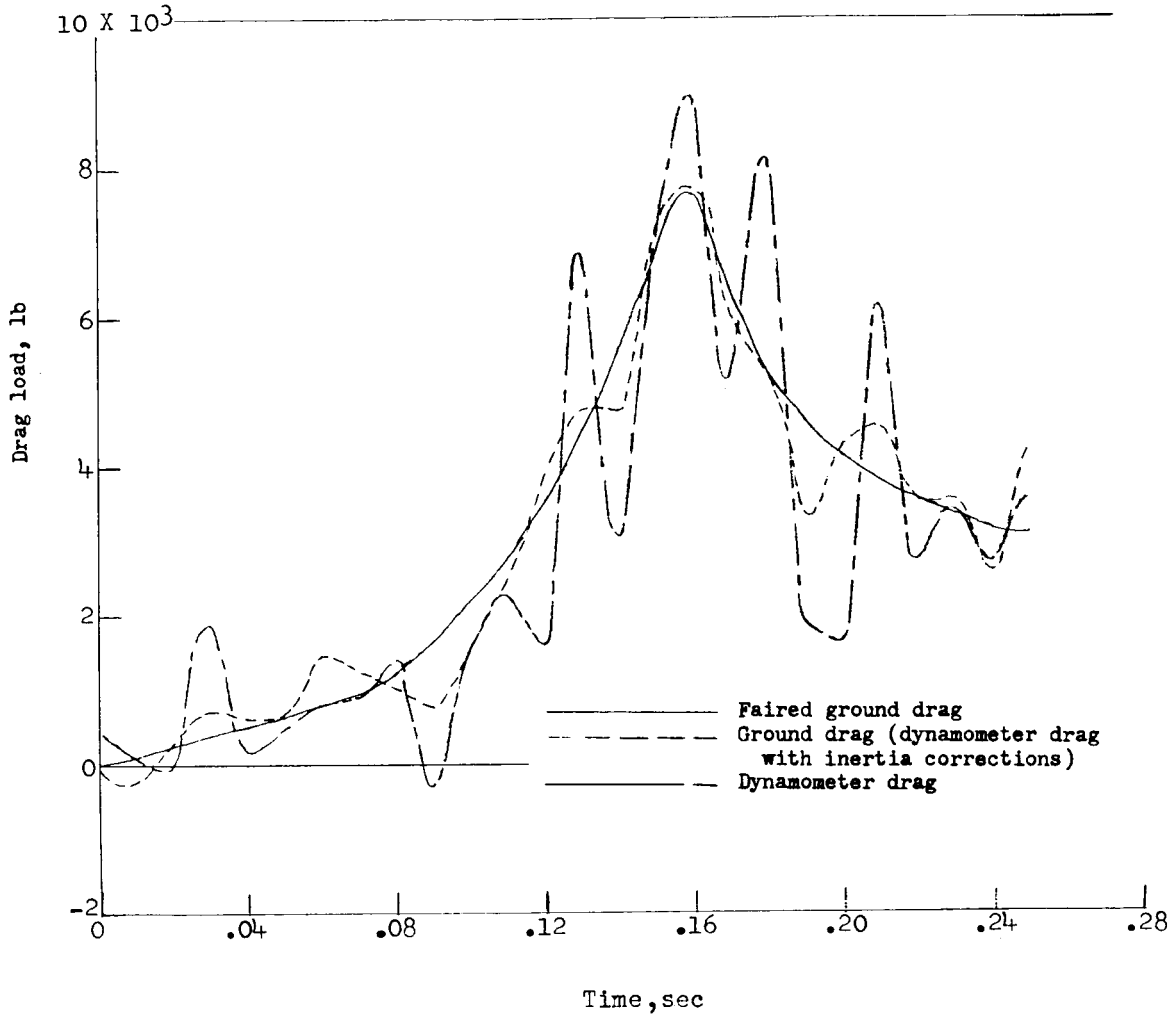

Figure 16.- Drag-force time histories obtained during test number 6. Dry surface; mat M9.

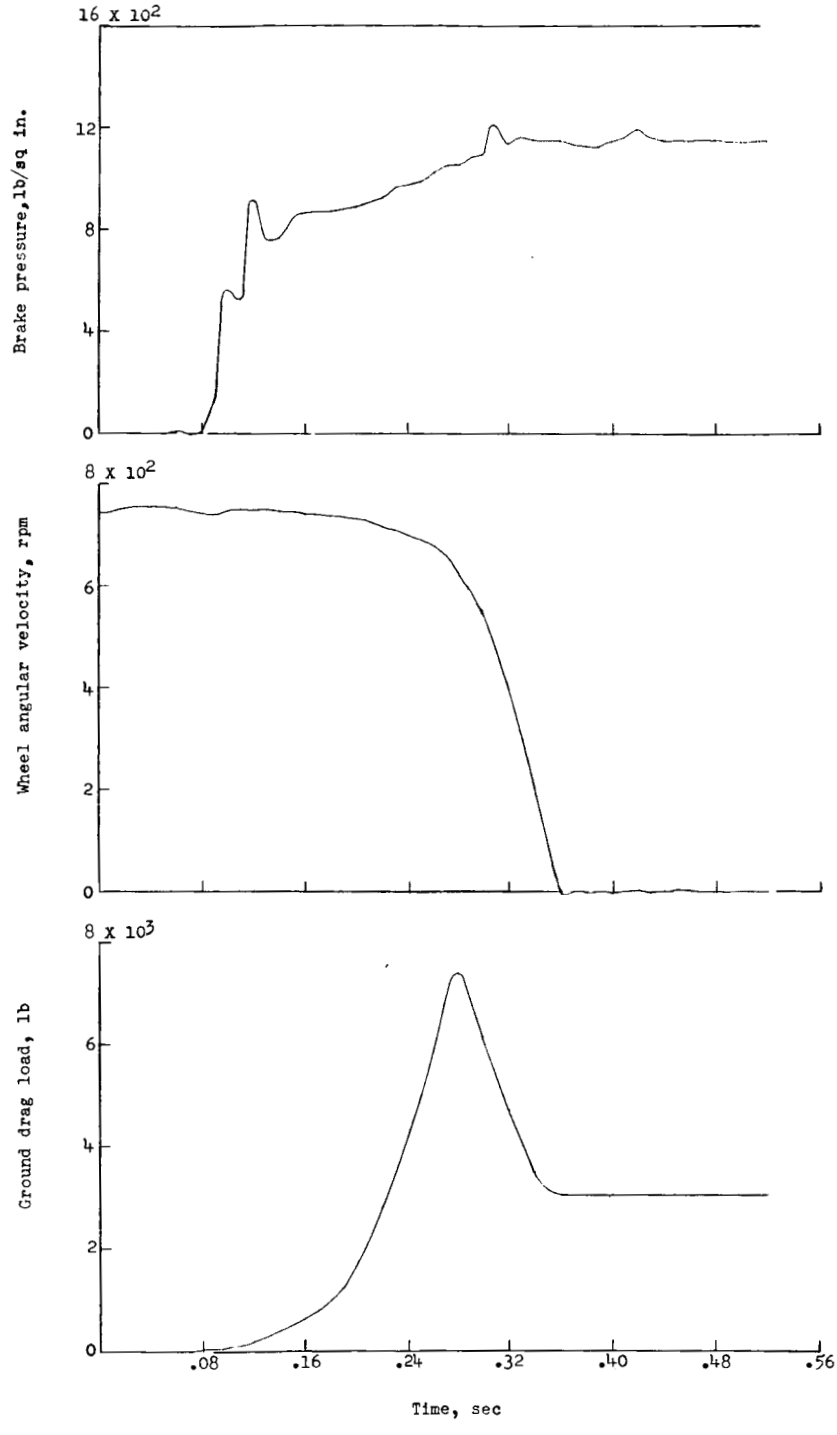

Figure 17.- Typical braking-test time-history plots. Test number 10. Mat M6.

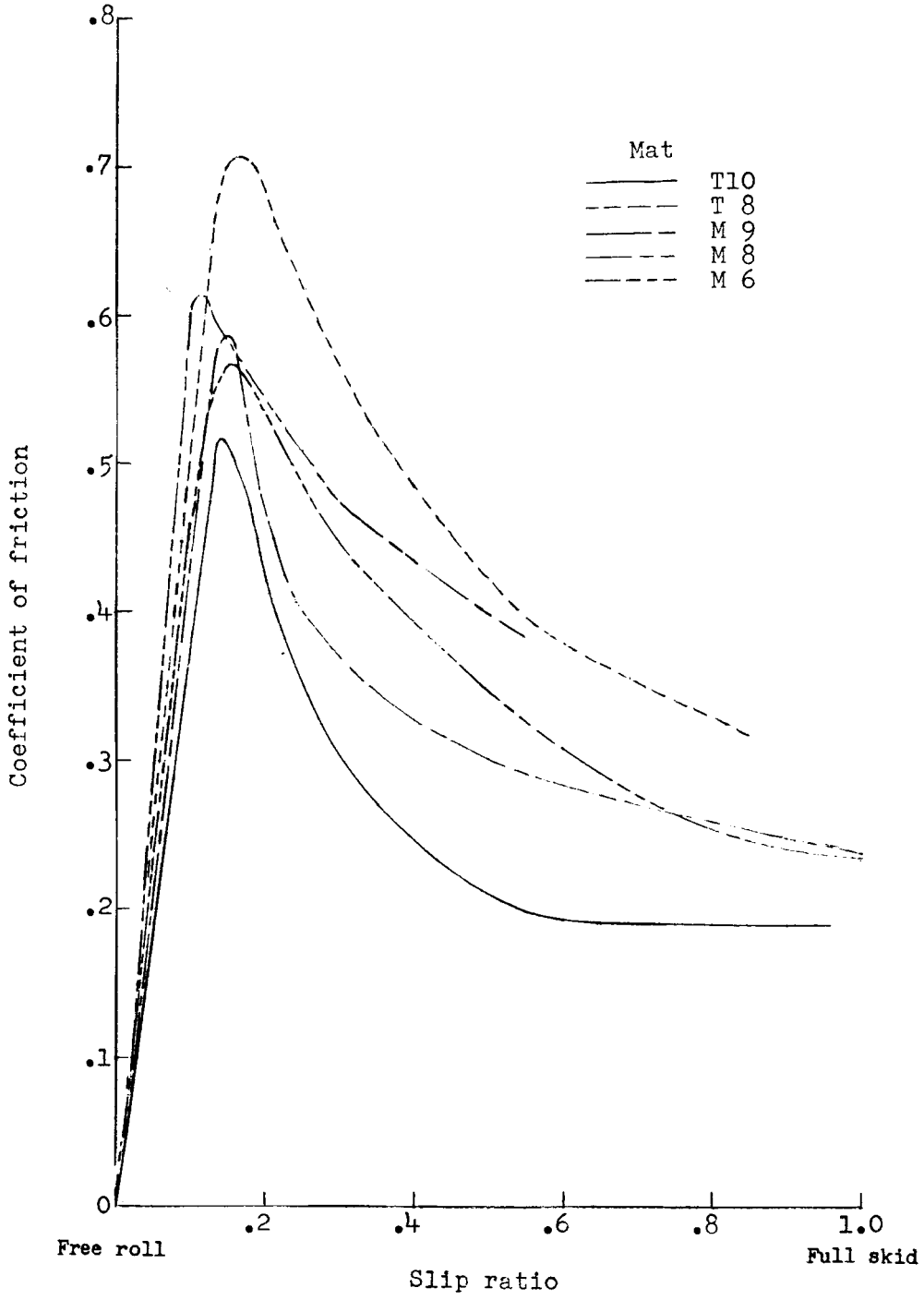

Figure 18.- Variation of coefficient of friction with slip ratio obtained during braking tests on dry metal landing mats. Static vertical load = 13,020 pounds.

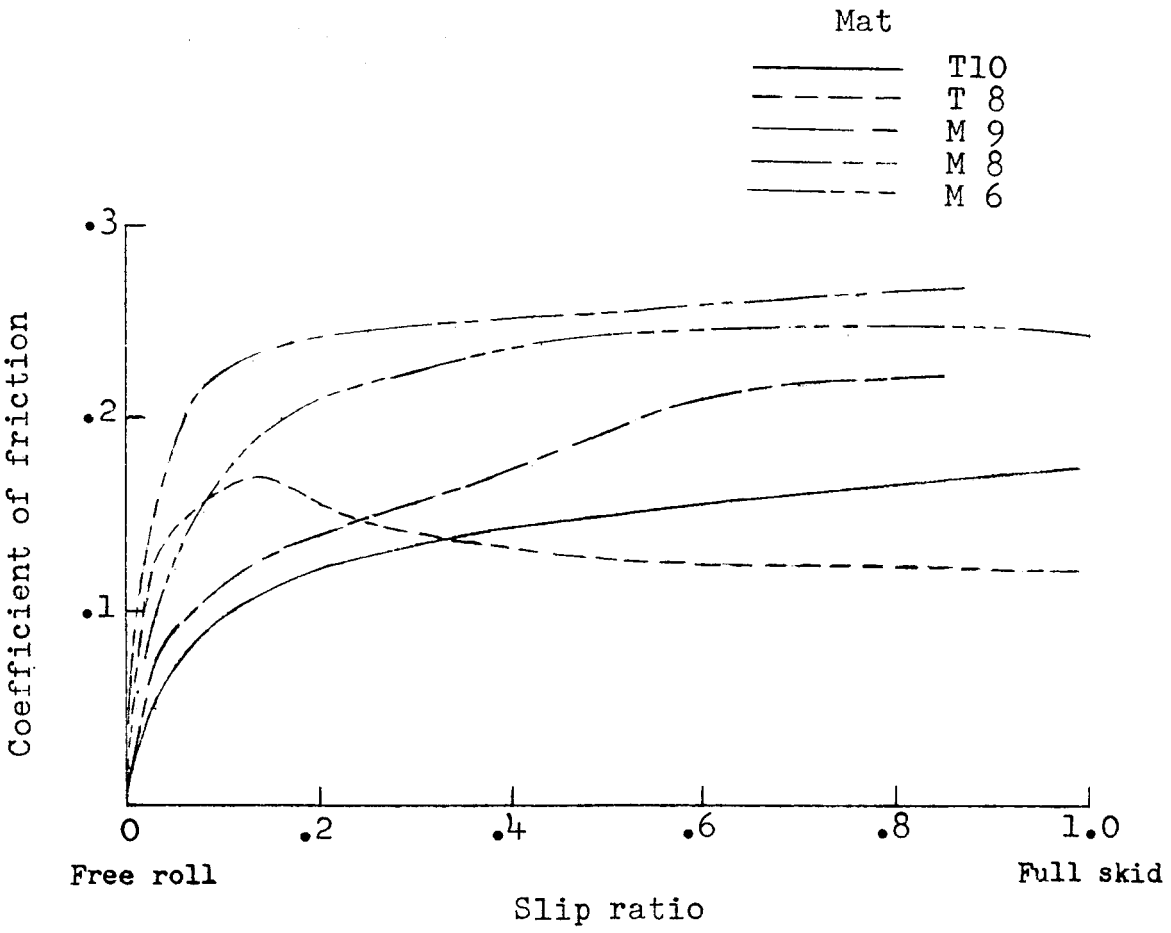

Figure 19.- Variation of coefficient of friction with slip ratio obtained during braking tests on wet metal landing mats. Static vertical load = 20,405 pounds.

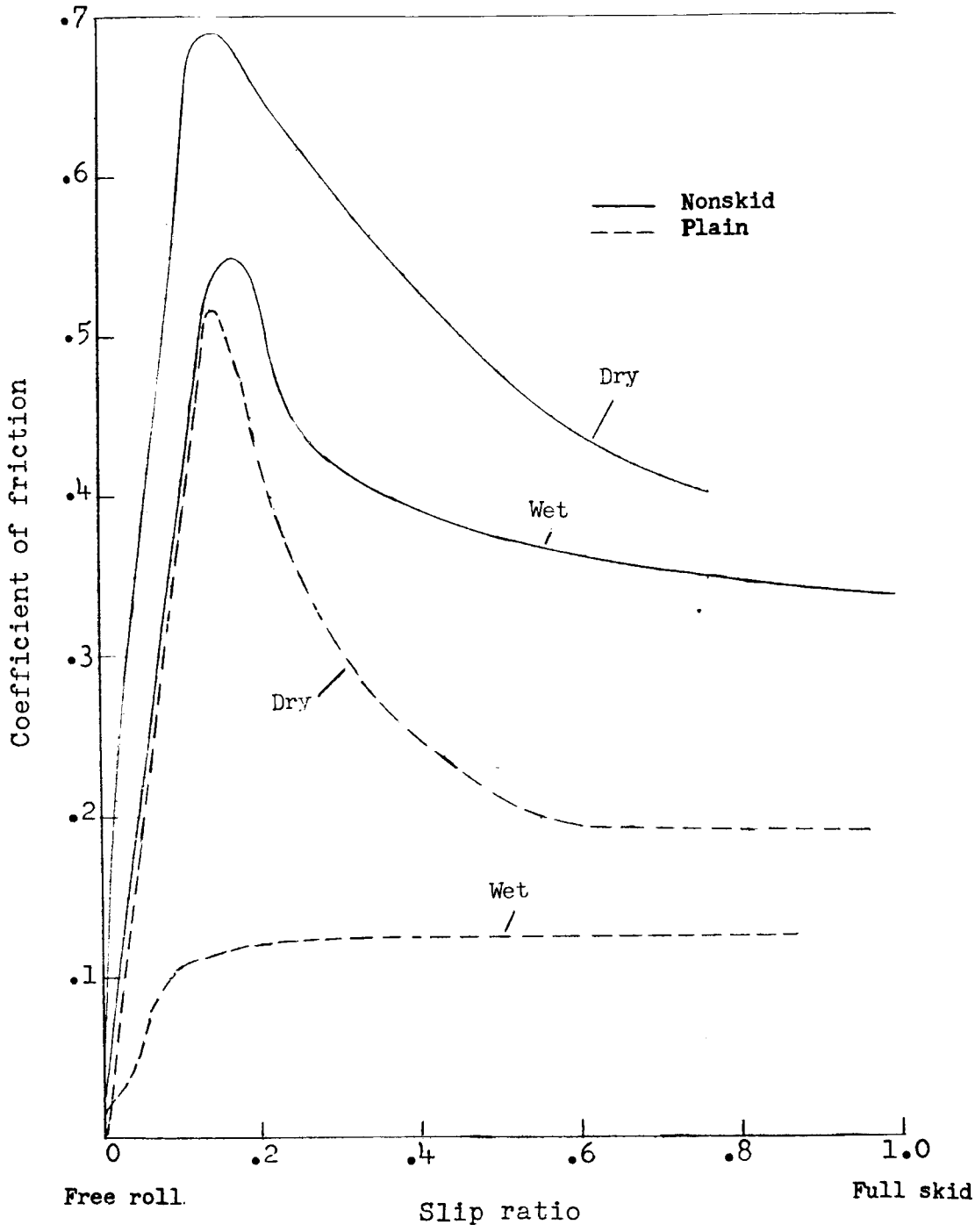

Figure 20.- Effect of nonskid surface coating on the coefficient of friction obtained during wet- and dry-surface braking tests on T10 landing mat. Static vertical load = 13,020 pounds.

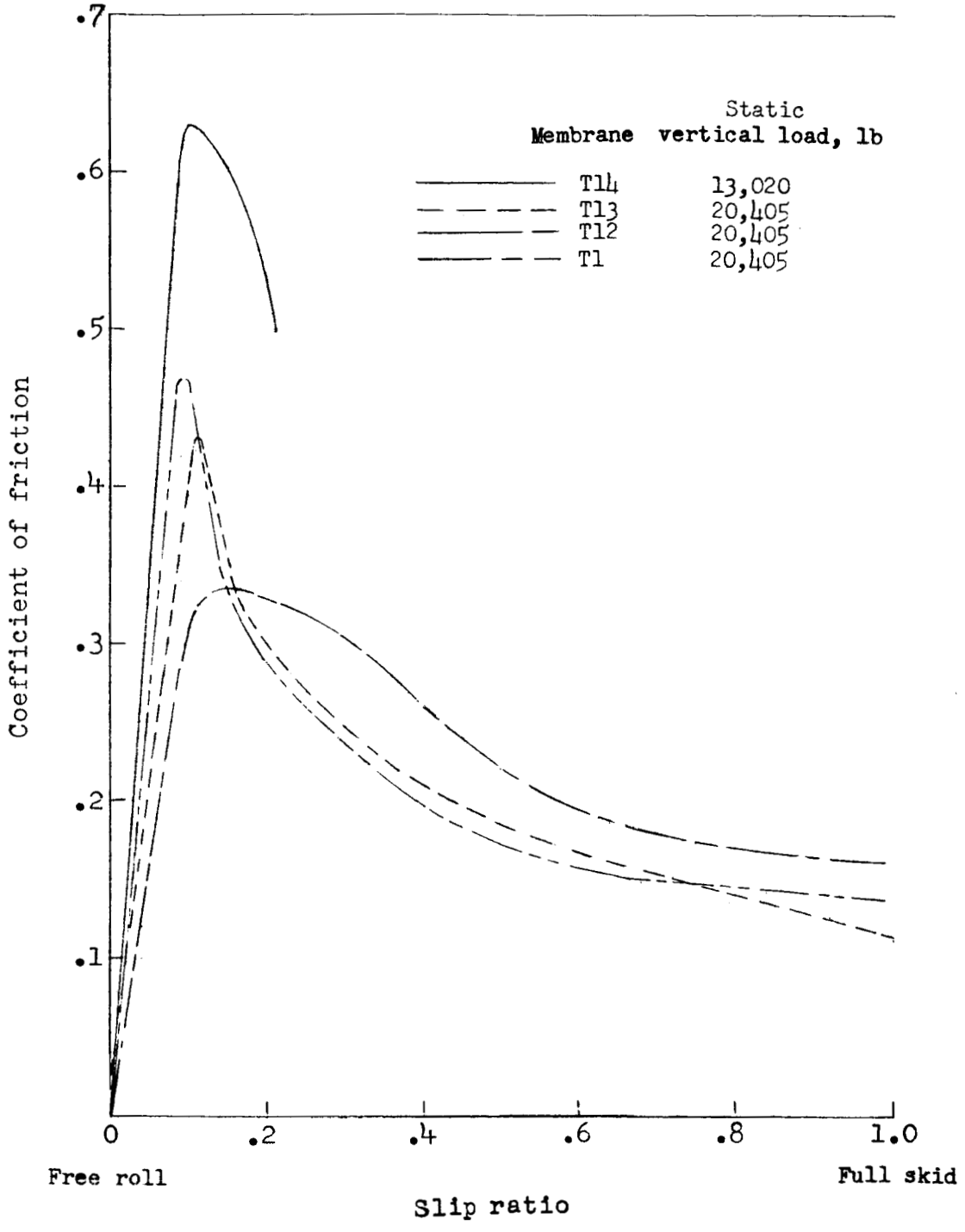

Figure 21.- Variation of coefficient of friction with slip ratio obtained during braking tests on dry membranes.

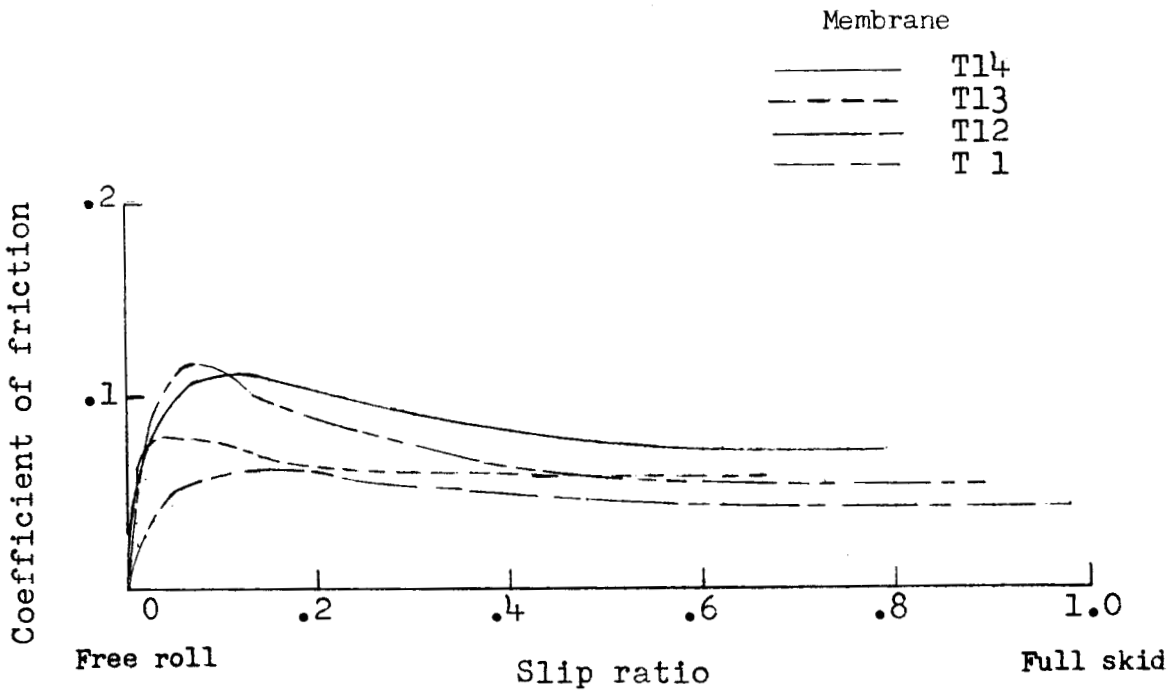

Figure 22.- Variation of coefficient of friction with slip ratio obtained during braking tests on wet membranes. Static vertical load = 20,405 pounds.

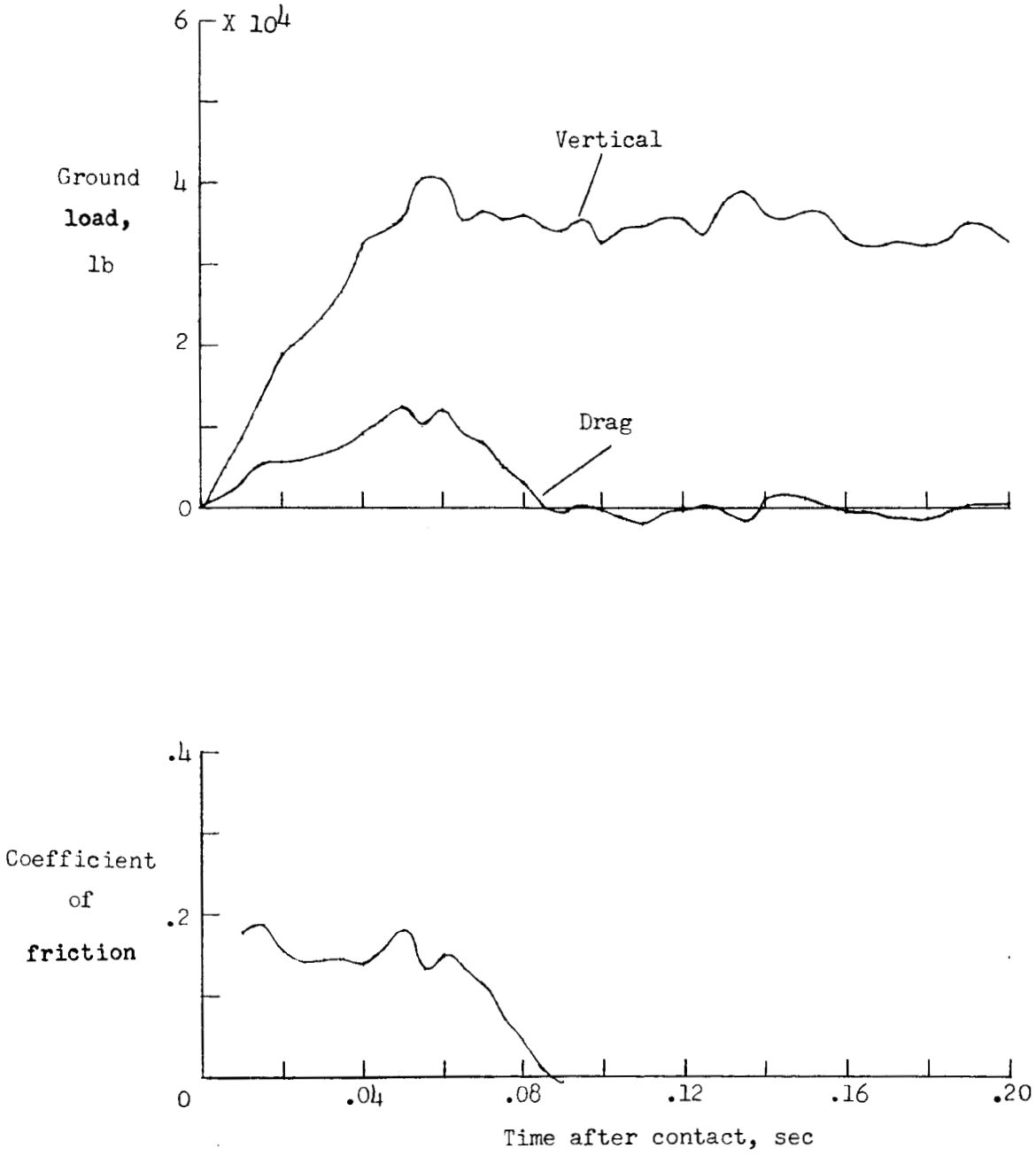

Figure 23.- Time histories of applied ground loads and coefficient of friction obtained during a landing impact on landing mat M6.

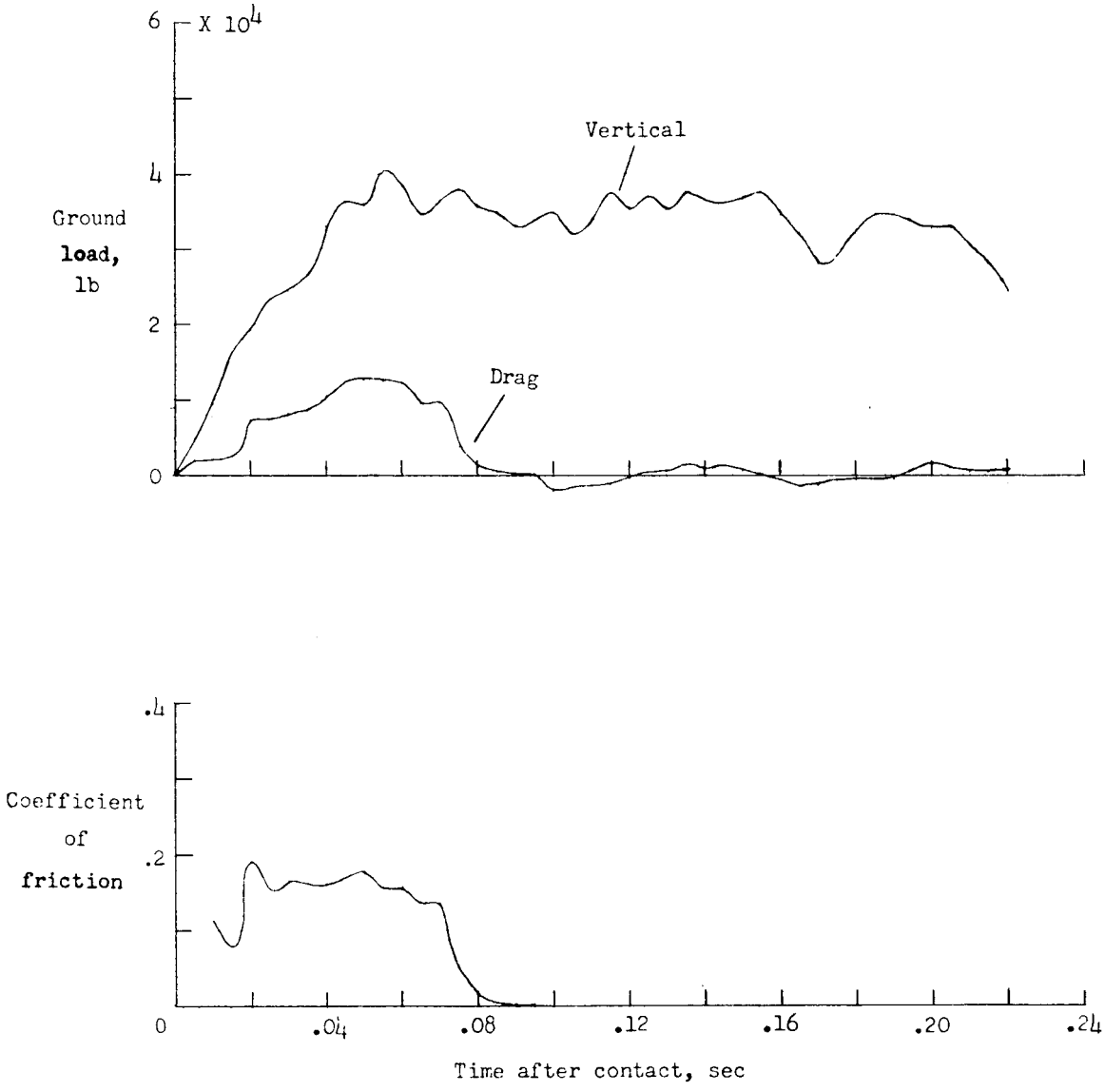

Figure 24.- Time histories of applied ground loads and coefficient of friction obtained during a landing impact on landing mat M8.

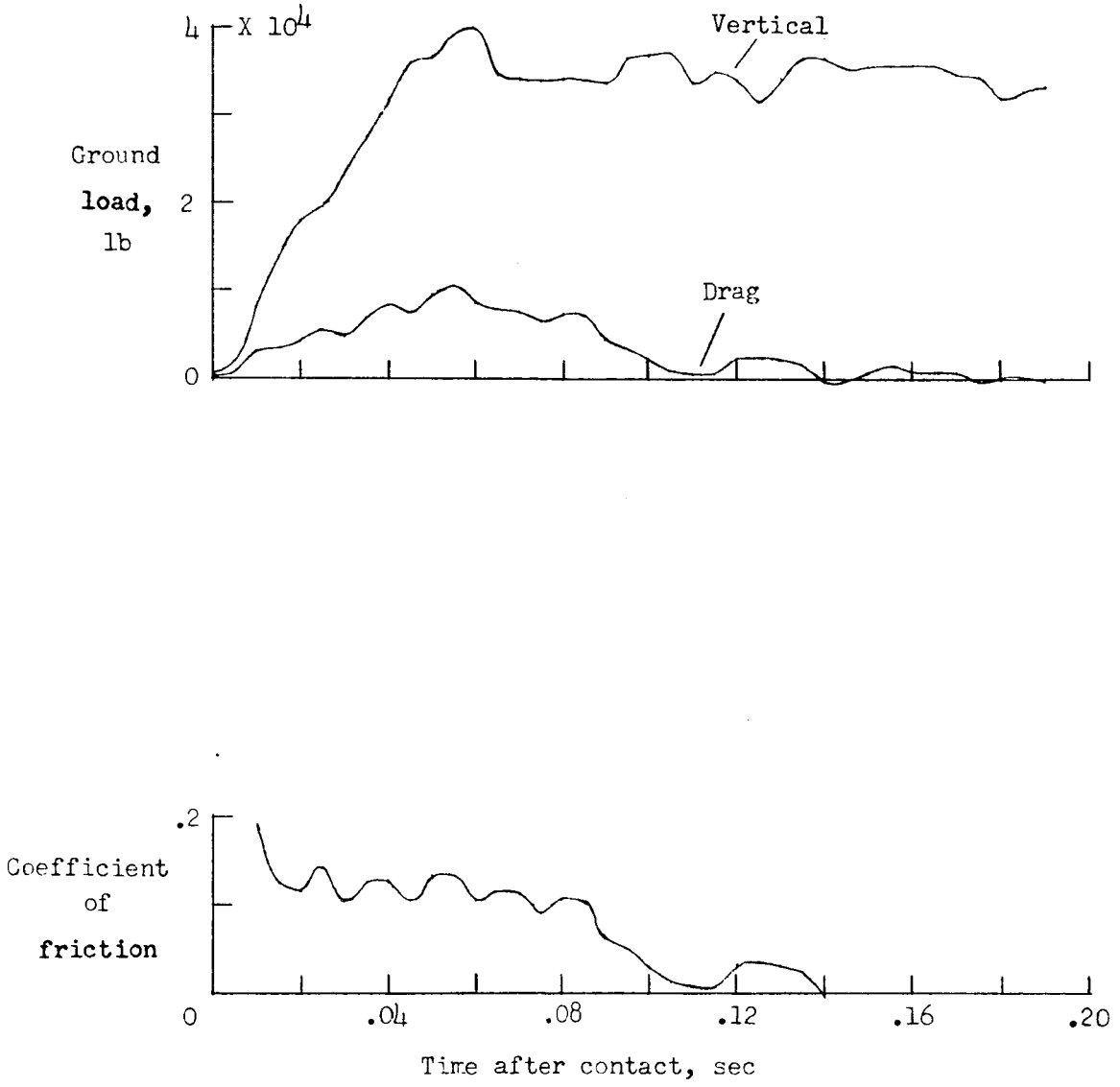

Figure 25.- Time histories of applied ground loads and coefficient of friction obtained during a landing impact on landing mat M9.

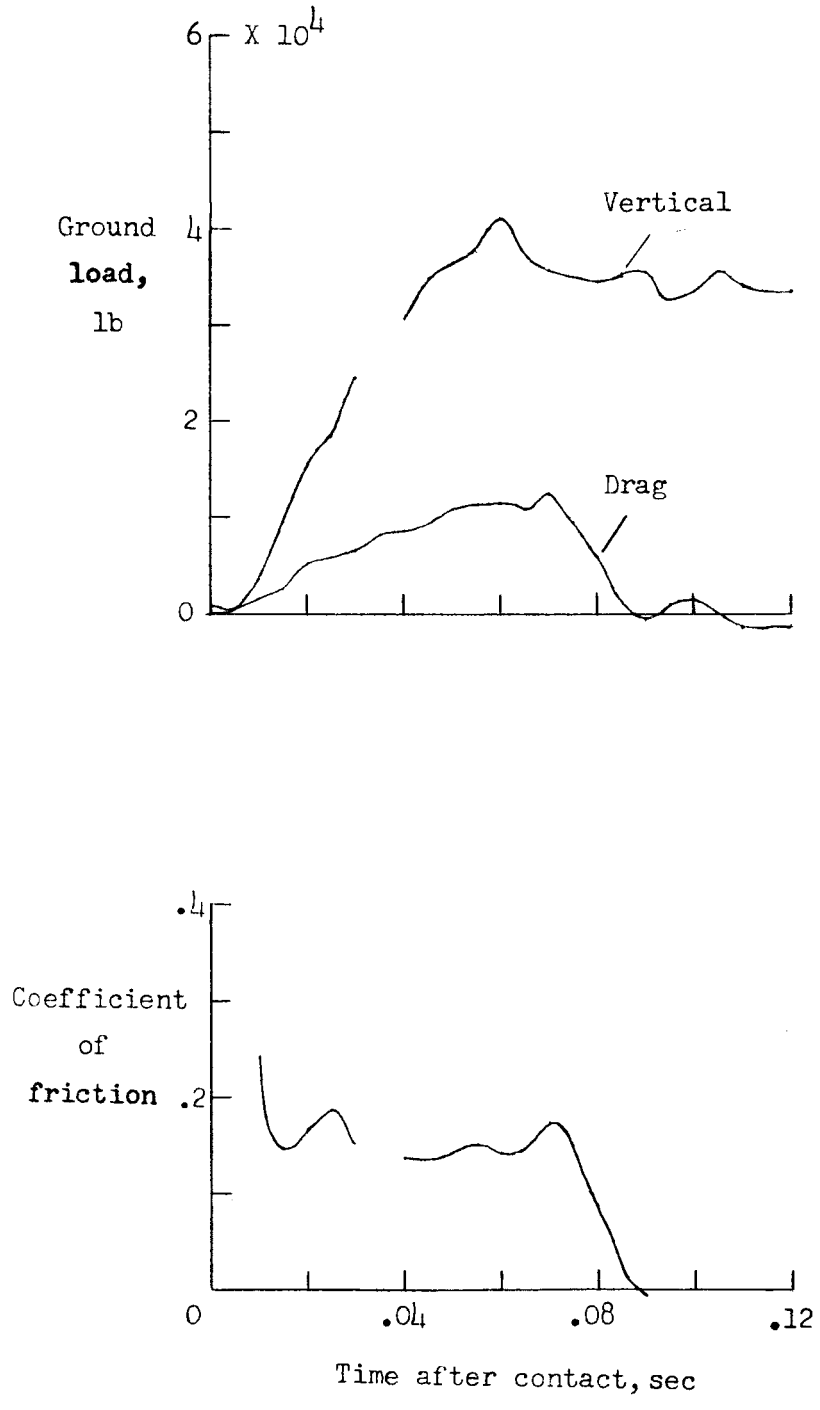

Figure 26.- Time histories of applied ground loads and coefficient of friction obtained during a landing impact on landing mat T8.

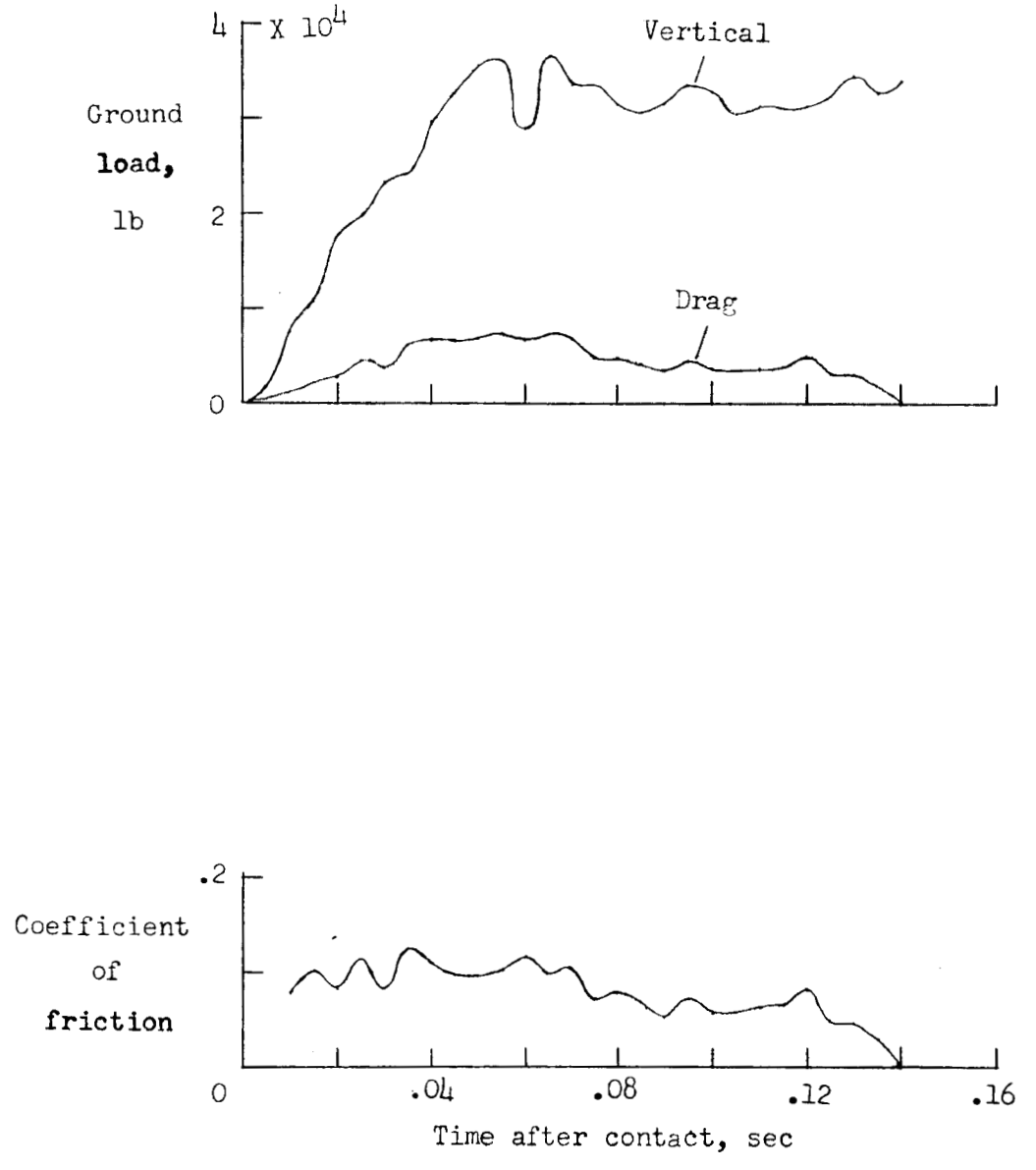

Figure 27.- Time histories of applied ground loads and coefficient of friction obtained during a landing impact on landing mat T10.

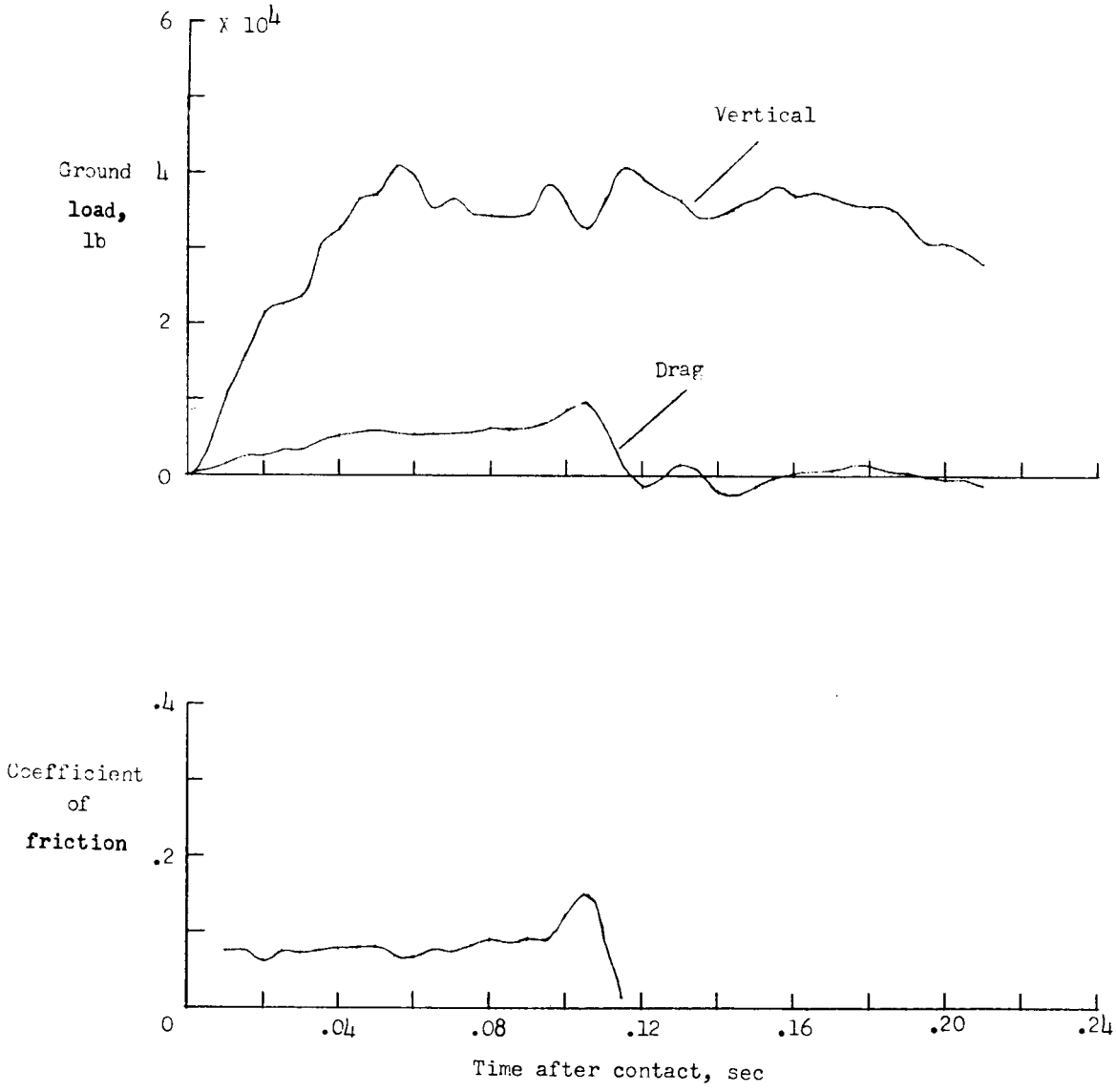

Figure 28.- Time histories of applied ground loads and coefficient of friction obtained during a landing impact on prefabricated membrane T14.

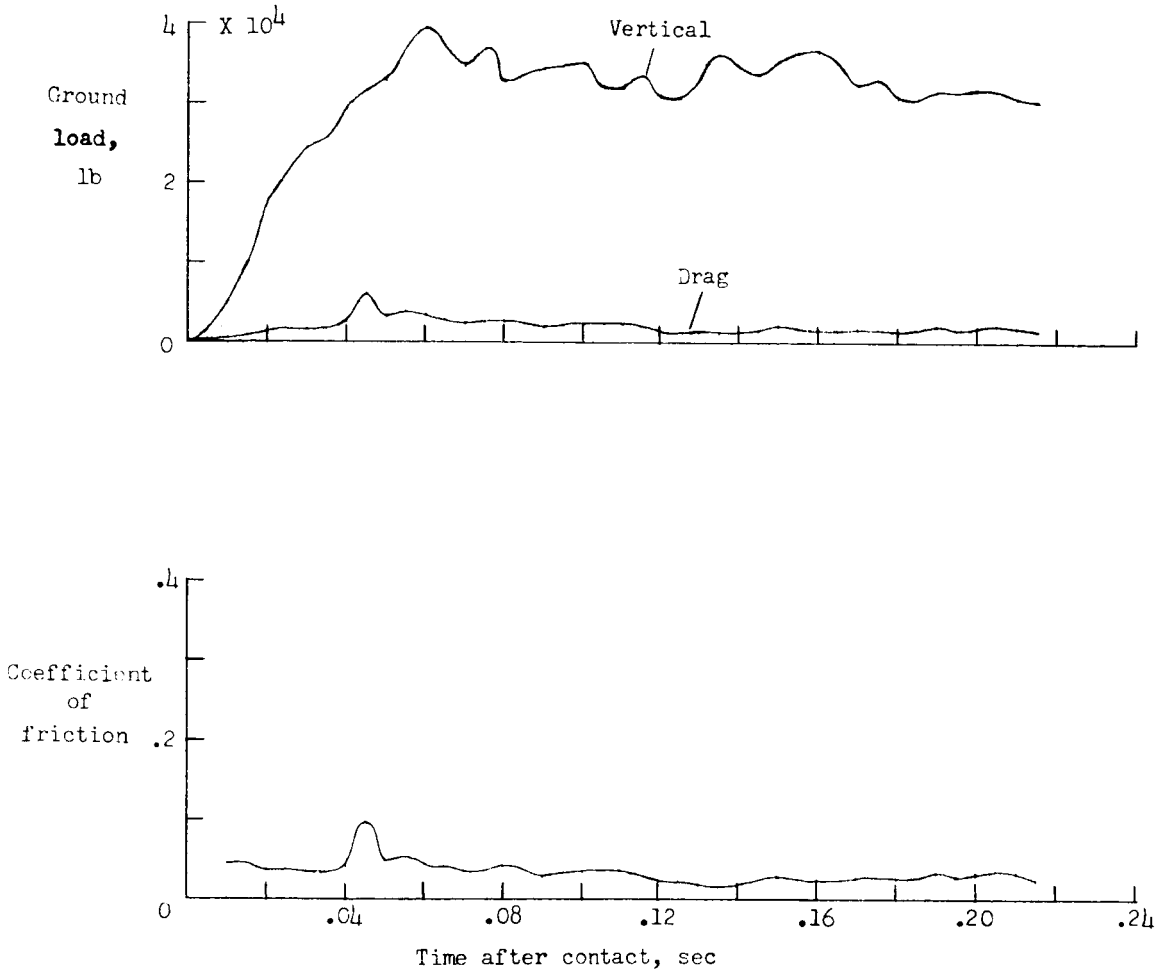

Figure 29.- Time histories of applied ground loads and coefficient of friction obtained during a landing impact on prefabricated membrane T13.

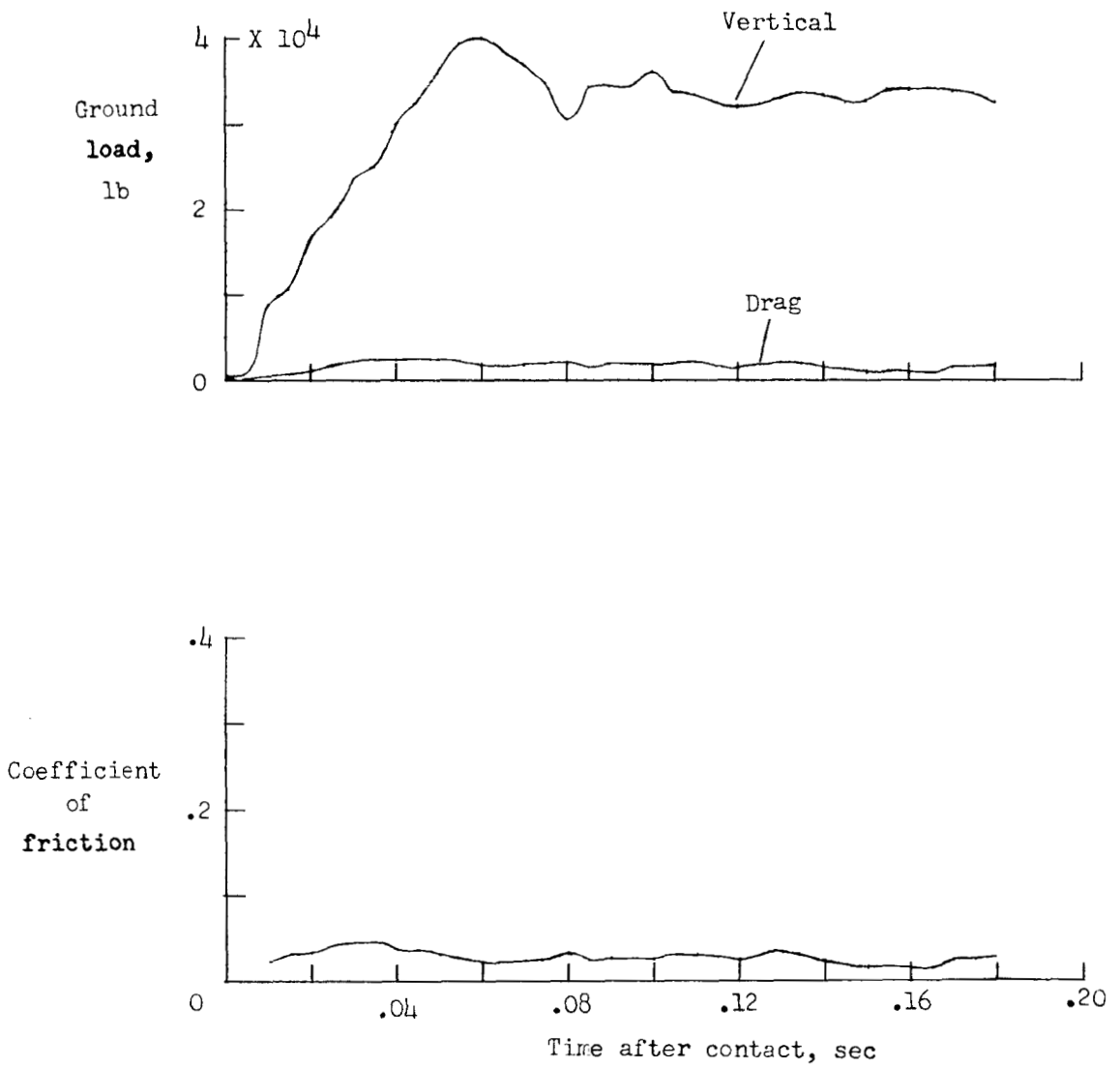

Figure 30.- Time histories of applied ground loads and coefficient of friction obtained during a landing impact on prefabricated membrane T12.

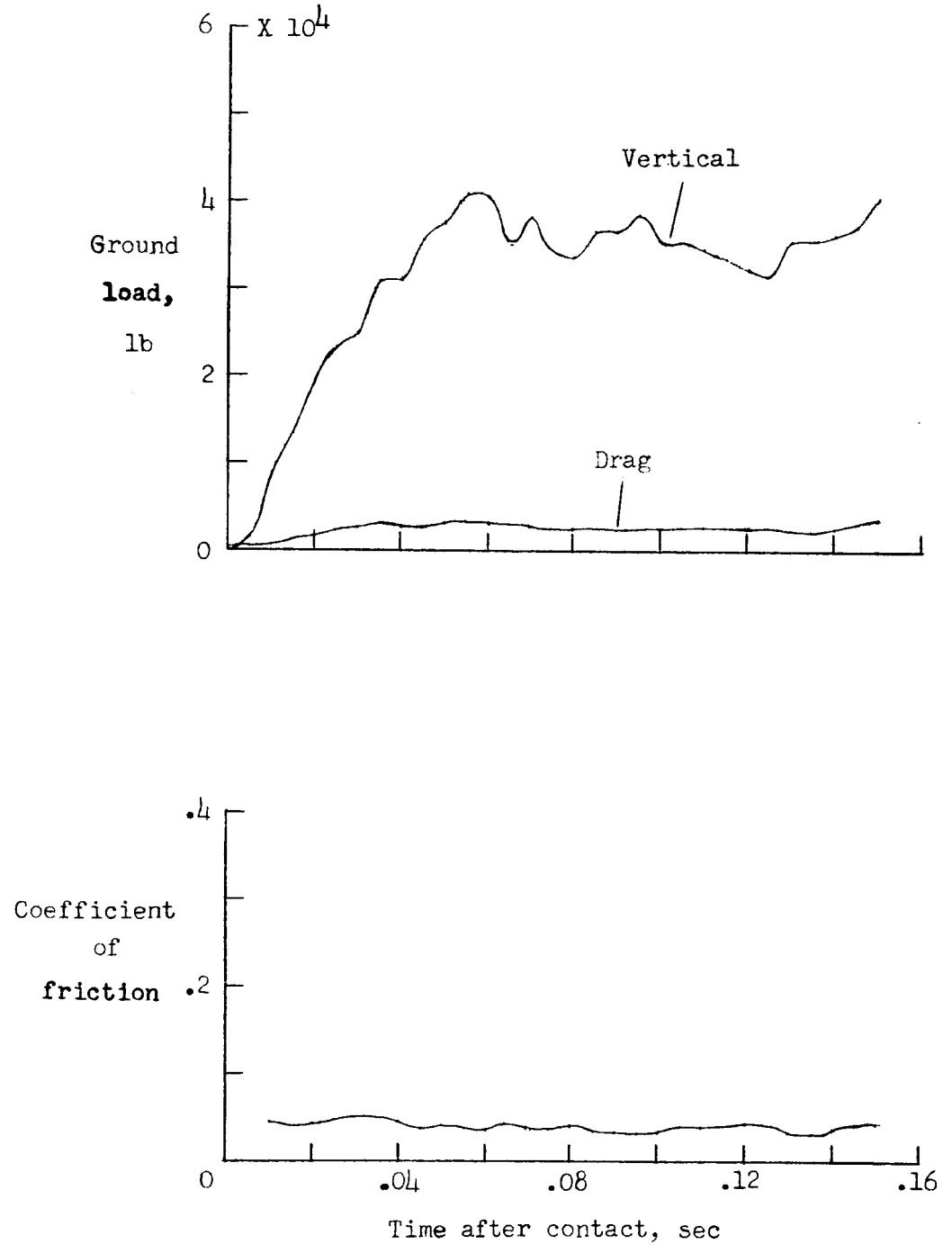

Figure 31.- Time histories of applied ground loads and coefficient of friction obtained during a landing impact on prefabricated membrane T1.